14 CP violation and weak hadronic interactions

CP violation is an essential part of our understanding of both particle physics and the evolution of the early Universe. It is required to explain the observed dominance of matter over antimatter in the Universe. In the Standard Model, the only place where CP violating effects can be accommodated is in the weak interactions of quarks and leptons. This chapter describes the weak charged-current interactions of the quarks and concentrates on the observations of CP violation in the neutral kaon and B-meson systems. This is not an easy topic and it is developed in several distinct stages. The detailed quantum mechanical derivations of the mixing of neutral meson states are given in two starred sections.

14.1 CP violation in the early Universe

The atoms in our local region of the Universe are formed from electrons, protons and neutrons rather than their equivalent antiparticles. The possibility that there are galaxies and/or regions of space dominated by antimatter can be excluded by the astronomical searches for photons from the e^+e^- annihilation process that would occur at the interfaces between matter and antimatter dominated regions of the Universe. The predominance of matter is believed to have arisen in the early evolution of the Universe.

In the early Universe, when the thermal energy $k_B T$ was large compared to the masses of the hadrons, there were an equal number of baryons and antibaryons. The baryons and antibaryons were initially in thermal equilibrium with the soup of relatively high-energy photons that pervaded the early Universe, through processes such as

$$\gamma + \gamma \rightleftharpoons p + \bar{p}. \tag{14.1}$$

As the Universe expanded, its temperature decreased as did the mean energy of the photons. At some point, the forward reaction of (14.1) effectively ceased. Furthermore, with the expansion, the number density of baryons and antibaryons also decreased and eventually became sufficiently low that annihilation processes such

as the backward reaction of (14.1) became very rare. At this point in time, the number of baryons and antibaryons in the Universe was effectively fixed. This process is known as Big Bang baryogenesis. The calculations of the thermal freeze out of the baryons *without* CP violation predict equal number densities of baryons and antibaryons, $n_{\mathrm{B}} = n_{\overline{\mathrm{B}}}$, and a baryon to photon number density ratio of

$$n_{\mathrm{B}} = n_{\overline{\mathrm{B}}} \sim 10^{-18} n_{\gamma}.$$

This prediction is in contradiction with the observed matter-dominated Universe, where the baryon–antibaryon asymmetry, which can be inferred from the relative abundances of light isotopes formed in the process of Big Bang nucleosynthesis, is

$$\frac{n_{\mathrm{B}} - n_{\overline{\mathrm{B}}}}{n_{\gamma}} \sim 10^{-9}.$$

Broadly speaking, to generate this asymmetry, for every 10^9 antibaryons in the early Universe there must have been $10^9 + 1$ baryons, which annihilated to give $O(10^9)$ photons, leaving 1 baryon.

To explain the observed matter–antimatter asymmetry in the Universe, three conditions, originally formulated by Sakharov (1967), must be satisfied. In the early Universe there must have been: (i) baryon number violation such that $n_{\mathrm{B}} - n_{\overline{\mathrm{B}}}$ is not constant; (ii) C and CP violation, because if CP is conserved, for every reaction that creates a net number of baryons over antibaryons there would be a CP conjugate reaction generating a net number of antibaryons over baryons; and (iii) departure from thermal equilibrium, since in thermal equilibrium any baryon number violating process will be balanced by the inverse reaction. The Standard Model of particle physics provides the possibility of CP violation in the weak interactions of quarks and leptons. To date, CP violation has only been observed in the quark sector, where many detailed measurements have been made. Despite the clear observations of CP violating effects in the weak interactions of quarks, this is not sufficient to explain the matter–antimatter asymmetry in the Universe and ultimately another source needs to be identified.

14.2 The weak interactions of quarks

In Section 12.1, it was shown that there is a universal coupling strength of the weak interaction to charged leptons and the corresponding neutrino weak eigenstates; $G_{\mathrm{F}}^{(\mathrm{e})} = G_{\mathrm{F}}^{(\mu)} = G_{\mathrm{F}}^{(\tau)}$. The strength of the weak interaction for quarks can be determined from the study of nuclear β-decay, where $|\mathcal{M}|^2 \propto G_{\mathrm{F}}^{(\mathrm{e})} G_{\mathrm{F}}^{(\beta)}$ and $G_{\mathrm{F}}^{(\beta)}$ gives the coupling at the weak interaction vertex of the quarks in Figure 14.1. From the observed β-decay rates for superallowed nuclear transitions, the strength of the

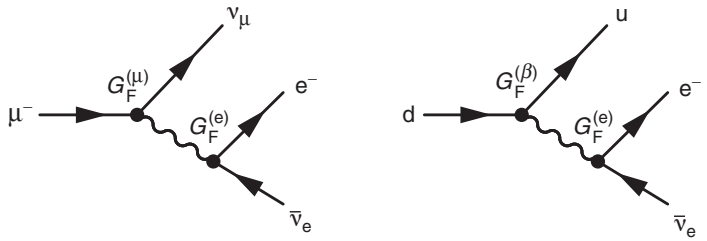

Fig. 14.1 The lowest-order Feynman diagrams for μ^--decay and the underlying quark-level process in nuclear β^--decay.

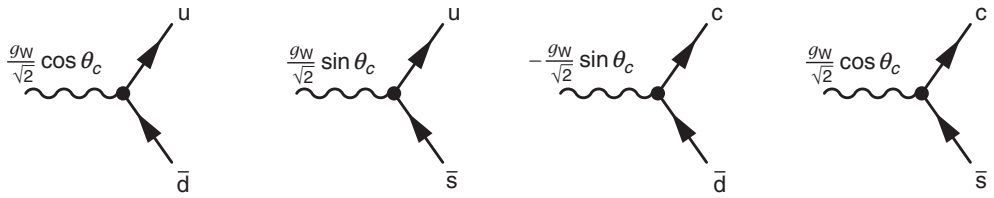

Fig. 14.2 The weak interaction couplings of the d, s, u and c in terms of the Cabibbo angle, θ_c.

coupling at the ud quark weak interaction vertex is found to be 5% smaller than that at the $\mu^-\nu_\mu$ vertex,

$$G_F^{(\mu)} = (1.166\,3787 \pm 0.000\,0006) \times 10^{-5}\,\text{GeV}^{-2},$$
$$G_F^{(\beta)} = (1.1066 \pm 0.0011) \times 10^{-5}\,\text{GeV}^{-2}.$$

Furthermore, different coupling strengths are found for the ud and us weak charged-current vertices. For example, the measured decay rate for $K^-(u\bar{s}) \rightarrow \mu^-\bar{\nu}_\mu$ compared to that of $\pi^-(u\bar{d}) \rightarrow \mu^-\bar{\nu}_\mu$ is approximately a factor 20 smaller than would be expected for a universal weak coupling to the quarks. These observations were originally explained by the Cabibbo hypothesis. In the Cabibbo hypothesis, the weak interactions of quarks have the same strength as the leptons, but the weak eigenstates of quarks differ from the mass eigenstates. The weak eigenstates, labelled d′ and s′, are related to the mass eigenstates, d and s, by the unitary matrix,

$$\begin{pmatrix} d' \\ s' \end{pmatrix} = \begin{pmatrix} \cos\theta_c & \sin\theta_c \\ -\sin\theta_c & \cos\theta_c \end{pmatrix} \begin{pmatrix} d \\ s \end{pmatrix}, \tag{14.2}$$

where θ_c is known as the Cabibbo angle. This idea is very similar to the two-flavour mixing of the neutrino mass and weak eigenstates encountered in Section 13.4. In the Cabibbo model, the weak interactions of quarks are described by ud′ and cs′ couplings, shown in Figure 14.2.

Nuclear β-decay involves the weak coupling between u and d quarks. Therefore, with the Cabibbo hypothesis, β-decay matrix elements are proportional to $g_W \cos\theta_c$ and decay rates are proportional to $G_F \cos^2\theta_c$. Similarly, the matrix

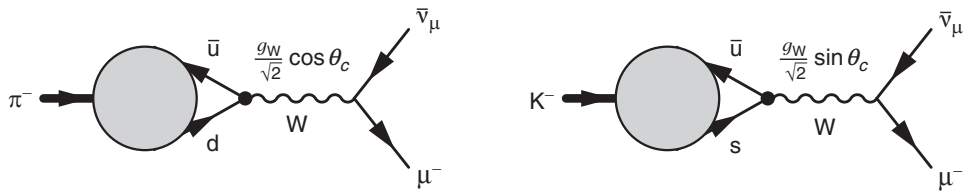

Fig. 14.3 The main decay modes of the π^- and K^-.

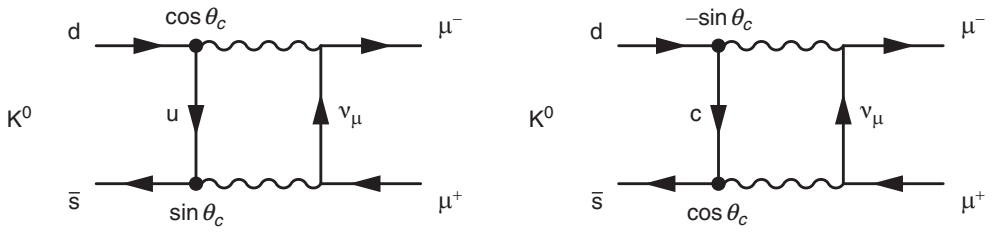

Fig. 14.4 Two box diagrams for the decay $K_L \rightarrow \mu^+\mu^-$. The distinction between the K_L and the K^0 is described in Section 14.4.

elements for the decays $K^- \rightarrow \mu^-\bar{\nu}_\mu$ and $\pi^- \rightarrow \mu^-\bar{\nu}_\mu$, shown in Figure 14.3, respectively include factors of $\cos\theta_c$ and $\sin\theta_c$. Consequently, after accounting for the difference in phase space, the K^- decay rate is suppressed by a factor of $\tan^2\theta_c$ relative to that for the π^-. The observed β-decay rates and the measured ratio of $\Gamma(K^-(u\bar{s}) \rightarrow \mu^-\bar{\nu}_\mu)$ to $\Gamma(\pi^-(ud) \rightarrow \mu^-\bar{\nu}_\mu)$ can be explained by the Cabibbo hypothesis with $\theta_c \simeq 13°$.

When the Cabibbo mechanism was first proposed, the charm quark had not been discovered. Since the Cabibbo mechanism allows for ud and us couplings, the flavour changing neutral-current (FCNC) decay of the neutral kaon $K_L \rightarrow \mu^+\mu^-$ can occur via the exchange of a virtual up-quark, as shown in the first box diagram of Figure 14.4. However, the observed branching ratio,

$$BR(K_L \rightarrow \mu^+\mu^-) = (6.84 \pm 0.11) \times 10^{-9},$$

is much smaller than expected from this diagram alone. This observation was explained by the GIM mechanism; see Glashow, Iliopoulos and Maiani (1970). In the GIM mechanism, which was formulated before the discovery of the charm quark, a postulated fourth quark coupled to the s′ weak eigenstate. In this case, the decay $K_L \rightarrow \mu^+\mu^-$ can also proceed via the exchange of a virtual charm quark, as shown in the second box diagram of Figure 14.4. The matrix elements for the two $K_L \rightarrow \mu^+\mu^-$ box diagrams are respectively

$$\mathcal{M}_u \propto g_W^4 \cos\theta_c \sin\theta_c \quad \text{and} \quad \mathcal{M}_c \propto -g_W^4 \cos\theta_c \sin\theta_c.$$

Because both diagrams give the same final state, the amplitudes must be summed

$$|\mathcal{M}|^2 = |\mathcal{M}_u + \mathcal{M}_c|^2 \approx 0.$$

The GIM mechanism therefore explains the smallness of the observed $K_L \to \mu^+\mu^-$ branching ratio. The cancellation is not exact because of the different masses of the up and charm quarks.

14.3 The CKM matrix

The Cabibbo mechanism is naturally extended to the three generations of the Standard Model, where the weak interactions of quarks are described in terms of the unitary Cabibbo–Kobayashi–Maskawa (CKM) matrix. The weak eigenstates are related to the mass eigenstates by

$$\begin{pmatrix} \mathrm{d}' \\ \mathrm{s}' \\ \mathrm{b}' \end{pmatrix} = \begin{pmatrix} V_{\mathrm{ud}} & V_{\mathrm{us}} & V_{\mathrm{ub}} \\ V_{\mathrm{cd}} & V_{\mathrm{cs}} & V_{\mathrm{cb}} \\ V_{\mathrm{td}} & V_{\mathrm{ts}} & V_{\mathrm{tb}} \end{pmatrix} \begin{pmatrix} \mathrm{d} \\ \mathrm{s} \\ \mathrm{b} \end{pmatrix}. \tag{14.3}$$

Consequently, the weak charged-current vertices involving quarks are given by

$$-i\frac{g_{\mathrm{W}}}{\sqrt{2}}\,(\,\bar{\mathrm{u}},\,\bar{\mathrm{c}},\,\bar{\mathrm{t}}\,)\,\gamma^{\mu}\tfrac{1}{2}(1-\gamma^5)\begin{pmatrix} V_{\mathrm{ud}} & V_{\mathrm{us}} & V_{\mathrm{ub}} \\ V_{\mathrm{cd}} & V_{\mathrm{cs}} & V_{\mathrm{cb}} \\ V_{\mathrm{td}} & V_{\mathrm{ts}} & V_{\mathrm{tb}} \end{pmatrix}\begin{pmatrix} \mathrm{d} \\ \mathrm{s} \\ \mathrm{b} \end{pmatrix},$$

where, for example, d is a down-quark spinor and $\bar{\mathrm{u}}$ is the adjoint spinor for an up-quark. The relative strength of the interaction is defined by the relevant element of the CKM matrix. For example, the weak charged-current associated with the duW vertex shown in the top left plot of Figure 14.5 is

$$j^{\mu}_{\mathrm{du}} = -i\tfrac{g_{\mathrm{W}}}{\sqrt{2}}\,V_{\mathrm{ud}}\,\bar{\mathrm{u}}\gamma^{\mu}\tfrac{1}{2}(1-\gamma^5)\mathrm{d}.$$

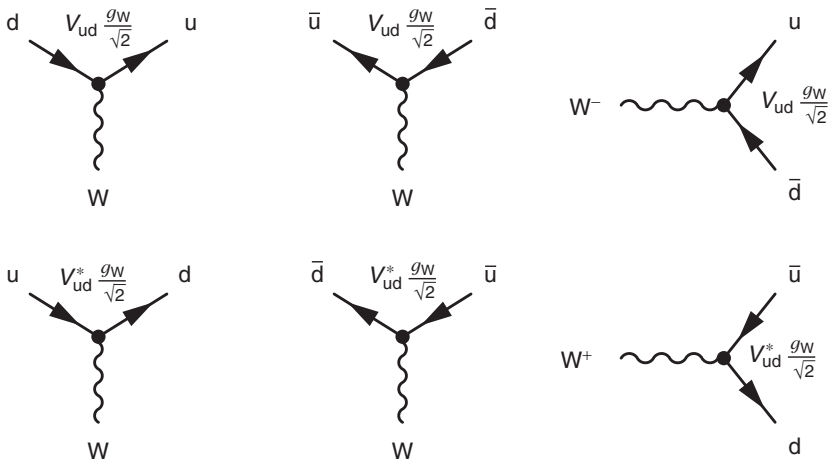

Fig. 14.5 The charged-current weak interaction vertices involving u and d quarks.

The CKM matrix is defined such that the associated vertex factor contains $V_{\rm ud}$ when the charge $-\frac{1}{3}$ quark enters the weak current as the spinor. If the charge $-\frac{1}{3}$ quark is represented by an adjoint spinor, $\overline{\rm d} = {\rm d}^\dagger\gamma^0$, the vertex factor from the CKM matrix is $V^*_{\rm ud}$. For example, the current associated with the vertex in the bottom left plot of Figure 14.5 is

$$j^\mu_{\rm ud} = -i\tfrac{g_{\rm W}}{\sqrt{2}}\, V^*_{\rm ud}\, \overline{\rm d}\gamma^\mu \tfrac{1}{2}(1-\gamma^5){\rm u}.$$

The CKM matrix, which is the analogous to the PMNS matrix for the weak interactions of leptons, is unitary and can be described by three rotation angles and a complex phase,

$$V_{\rm CKM} = \begin{pmatrix} V_{\rm ud} & V_{\rm us} & V_{\rm ub} \\ V_{\rm cd} & V_{\rm cs} & V_{\rm cb} \\ V_{\rm td} & V_{\rm ts} & V_{\rm tb} \end{pmatrix} = \begin{pmatrix} 1 & 0 & 0 \\ 0 & c_{23} & s_{23} \\ 0 & -s_{23} & c_{23} \end{pmatrix} \times \begin{pmatrix} c_{13} & 0 & s_{13}e^{-i\delta'} \\ 0 & 1 & 0 \\ -s_{13}e^{i\delta'} & 0 & c_{13} \end{pmatrix} \times \begin{pmatrix} c_{12} & s_{12} & 0 \\ -s_{12} & c_{12} & 0 \\ 0 & 0 & 1 \end{pmatrix}, \tag{14.4}$$

where $s_{ij} = \sin\phi_{ij}$ and $c_{ij} = \cos\phi_{ij}$.

Whilst the structure of the weak interactions of quarks and leptons is the same, the phenomenology is very different. Quarks do not propagate as free particles, but hadronise on a length scale of 10^{-15} m. Consequently, the final states of weak interactions involving quarks have to be described in terms of mesons or baryons. The observed hadronic states are composed of particular quark flavours and, therefore, it is the quark mass (flavour) eigenstates that form the observable quantities in hadronic weak interactions. Consequently, the nine individual elements of the CKM matrix can be measured separately. For example, $V_{\rm ud}$ is determined from superallowed nuclear β-decays,

$$|V_{\rm ud}| = \cos\theta_c = 0.974\ 25(22).$$

The weak coupling between the u and s quarks can be determined from the measured branching ratio of the ${\rm K}^0 \to \pi^-{\rm e}^+\nu_{\rm e}$ decay shown in Figure 14.6a,

$$|V_{\rm us}| = 0.225\ 2(9).$$

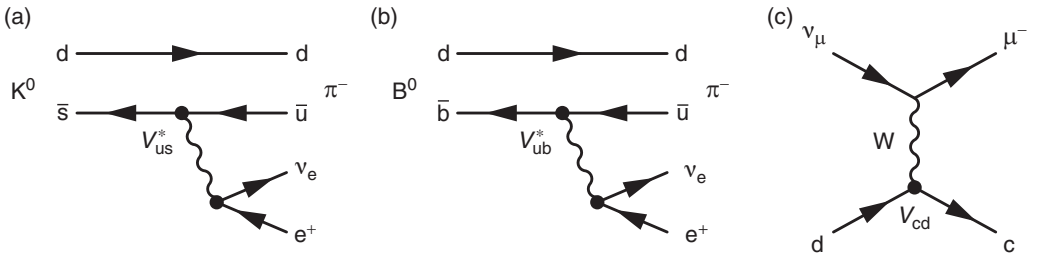

Fig. 14.6 The Feynman diagrams for a) ${\rm K}^0 \to \pi^-{\rm e}^+\nu_{\rm e}$, b) ${\rm B}^0 \to \pi^-{\rm e}^+\nu_{\rm e}$ and c) $\nu_\mu{\rm d} \to \mu^-{\rm c}$.

The large numbers of $B^0(d\bar{b})$ and $\overline{B}^0(b\bar{d})$ mesons produced at the BaBar and Belle experiments, described in Section 14.6.3, allow precise measurements of the branching ratios for decays such as $B^0 \to \pi^- e^+ \nu_e$, shown in Figure 14.6b. The measurements of the inclusive and exclusive branching ratios of the B-mesons imply

$$|V_{ub}| = (4.15 \pm 0.49) \times 10^{-3}.$$

The CKM matrix element V_{cs} can be determined from the leptonic decays of the $D_s^+(u\bar{s})$ meson, for example $D_s^+ \to \mu^+ \nu_\mu$, and V_{cb} can be determined from the semi-leptonic decay modes of B-mesons to final states with charm quarks, giving

$$|V_{cs}| = 1.006 \pm 0.023 \quad \text{and} \quad |V_{cb}| = (40.9 \pm 1.1) \times 10^{-3}.$$

The CKM matrix element V_{cd} is most precisely measured in neutrino–nucleon scattering, $\nu_\mu d \to \mu^- c$, shown in Figure 14.6c. The final-state charm quark can be identified from its semi-leptonic decay $c \to s\mu^+\nu_\mu$, which gives an experimental signature of a pair of oppositely charged muons, one from the charm production process and one from its decay. The observed production rate of opposite sign muons in neutrino deep inelastic scattering gives

$$|V_{cd}| = 0.230(11).$$

The experimental situation for the CKM matrix elements involving top quarks is somewhat less clear. The observations of $B^0 \leftrightarrow \overline{B}^0$ oscillations, described in Section 14.6, can be interpreted in the Standard Model as measurements of

$$|V_{td}| = (8.4 \pm 0.6) \times 10^{-3} \quad \text{and} \quad |V_{ts}| = (42.9 \pm 2.6) \times 10^{-3}.$$

From the observed decay modes of the top quark at CDF and D0, it is known that the top quark decays predominantly via $t \to bW$ and therefore $|V_{tb}|$ is close to unity, although the current experimental error is at the 10% level.

In the Standard Model, the CKM matrix is unitary, $V^\dagger V = I$, which implies that

$$|V_{ud}|^2 + |V_{us}|^2 + |V_{ub}|^2 = 1, \tag{14.5}$$

$$|V_{cd}|^2 + |V_{cs}|^2 + |V_{cb}|^2 = 1, \tag{14.6}$$

$$|V_{td}|^2 + |V_{ts}|^2 + |V_{tb}|^2 = 1. \tag{14.7}$$

The measurements of the individual CKM matrix elements, described above, are consistent with these three unitarity relations. Assuming unitarity, further constraints can be placed on the less precisely determined CKM matrix elements, for example $|V_{tb}|^2 = 1 - |V_{ts}|^2 - |V_{tb}|^2$, which implies that $|V_{tb}| = 0.999$. With the unitarity constraints from (14.5)–(14.7), the experimental measurements can be interpreted as

$$\begin{pmatrix} |V_{ud}| & |V_{us}| & |V_{ub}| \\ |V_{cd}| & |V_{cs}| & |V_{cb}| \\ |V_{td}| & |V_{ts}| & |V_{tb}| \end{pmatrix} \approx \begin{pmatrix} 0.974 & 0.225 & 0.004 \\ 0.225 & 0.973 & 0.041 \\ 0.009 & 0.040 & 0.999 \end{pmatrix}. \tag{14.8}$$

Unlike the PMNS matrix of the lepton flavour sector, the off-diagonal terms in the CKM matrix are relatively small. This implies that the rotation angles between the quark mass and weak eigenstates in (14.4) are also small, $\phi_{12} = 13°$, $\phi_{23} = 2.3°$ and $\phi_{13} = 0.2°$. The smallness of these angles leads to the near diagonal form of the CKM matrix. Consequently, the weak interactions of quarks of different generations are suppressed relative to those of the same generation, ud, cs and tb. The suppression is largest for the couplings between first and third generation quarks, ub and td.

Because of the near diagonal nature of the CKM matrix, it is convenient to express it as an expansion in the relatively small parameter $\lambda = \sin\theta_c = 0.225$. In the widely used Wolfenstein parameterisation, the CKM matrix is written in terms of four real parameters, λ, A, ρ and η. To $O(\lambda^4)$ the CKM matrix then can be parameterised as

$$\begin{pmatrix} V_{ud} & V_{us} & V_{ub} \\ V_{cd} & V_{cs} & V_{cb} \\ V_{td} & V_{ts} & V_{tb} \end{pmatrix} = \begin{pmatrix} 1-\lambda^2/2 & \lambda & A\lambda^3(\rho - i\eta) \\ -\lambda & 1-\lambda^2/2 & A\lambda^2 \\ A\lambda^3(1-\rho-i\eta) & -A\lambda^2 & 1 \end{pmatrix} + O(\lambda^4). \tag{14.9}$$

In the Wolfenstein parameterisation, the complex components of the CKM matrix reside only in V_{ub} and V_{td} (although if higher-order terms are included, V_{cd} and V_{ts} also have a small complex components that are proportional to λ^5). For CP to be violated in the quark sector, the CKM matrix must contain an irreducible complex phase and this corresponds to η being non-zero. The experimental measurements of branching ratios only constrain the magnitudes of the individual CKM matrix elements, and do not provide any information about this complex phase. To constrain η and ρ separately, measurements that are sensitive to the amplitudes, rather than amplitudes squared are required. Such measurements can be made in the neutral kaon and neutral B-mesons systems.

14.4 The neutral kaon system

The first experimental observation of CP violation was made in the neutral kaon system. The $K^0(d\bar{s})$ and $\overline{K}^0(s\bar{d})$ are the lightest mesons containing strange quarks. They are produced copiously in strong interactions, for example in processes

$$\pi^-(d\bar{u}) + p(uud) \to \Lambda(uds) + K^0(d\bar{s}),$$
$$p(uud) + \bar{p}(\bar{u}\,\bar{u}\bar{d}) \to K^+(u\bar{s}) + \overline{K}^0(s\bar{d}) + \pi^-(d\bar{u}).$$

The K^0 and $\overline{K}^0$ are the eigenstates of the strong interaction and are referred to as the flavour states. Since they are the lightest hadrons containing strange quarks, the K^0 and $\overline{K}^0$ can decay only by the weak interaction. Because the neutral kaons

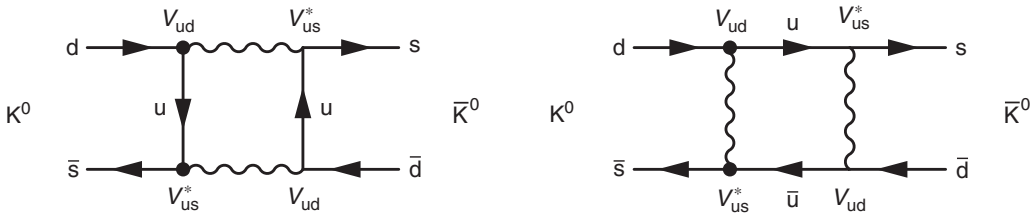

Fig. 14.7 Two box diagrams for $K^0 \leftrightarrow \overline{K}^0$ mixing. There are corresponding diagrams involving all nine combinations of virtual up, charm and top quarks.

are relatively light, $m(K) = 498\,\text{MeV}$, only decays to final states with either leptons (e/μ) or pions are kinematically allowed. The weak interaction also provides a mechanism whereby the neutral kaons can mix through the $K^0 \leftrightarrow \overline{K}^0$ box diagrams shown in Figure 14.7.

In quantum mechanics, the physical states are the eigenstates of the free-particle Hamiltonian. These are the stationary states introduced in Section 2.3.3. Until now, independent stationary states have been used to describe each type of particle. Here however, because of the $K^0 \leftrightarrow \overline{K}^0$ mixing process, a neutral kaon that is produced as a K^0 will develop a $\overline{K}^0$ component. For this reason, the K^0–$\overline{K}^0$ system has to be considered as a whole. The physical neutral kaon states are the stationary states of the *combined* Hamiltonian of the K^0–$\overline{K}^0$ system, including the weak interaction mixing Hamiltonian. Consequently, the neutral kaons propagate as linear combinations of the K^0 and $\overline{K}^0$. These physical states are known as the K-short (K_S) and the K-long (K_L). The K_S and K_L are observed to have very similar masses, $m(K_S) \approx m(K_L) \approx 498\,\text{MeV}$, but quite different lifetimes,

$$\tau(K_S) = 0.9 \times 10^{-10}\,\text{s} \quad \text{and} \quad \tau(K_L) = 0.5 \times 10^{-7}\,\text{s}.$$

If CP were an exact symmetry of the weak interaction, the K_S and K_L would be equivalent to the CP eigenstates of the neutral kaon system (the proof of this statement is given in Section 14.4.3). The CP states can be identified by considering the action of the parity and charge conjugation operators on the neutral kaons. The flavour eigenstates, $K^0(d\bar{s})$ and $\overline{K}^0(s\bar{d})$, have spin-parity $J^P = 0^-$ and therefore

$$\hat{P}|K^0\rangle = -|K^0\rangle \quad \text{and} \quad \hat{P}|\overline{K}^0\rangle = -|\overline{K}^0\rangle.$$

The K^0 and $\overline{K}^0$ are not eigenstates of the charge conjugation operator $\hat{C}$ that has the effect of replacing particles with antiparticles and vice versa. However, since they are neutral particles with opposite flavour content, one can write

$$\hat{C}|K^0(d\bar{s})\rangle = e^{i\zeta}|\overline{K}^0(\bar{d}s)\rangle \quad \text{and} \quad \hat{C}|\overline{K}^0(\bar{d}s)\rangle = e^{-i\zeta}|K^0(d\bar{s})\rangle,$$

where ζ is an unobservable phase factor, which is conventionally[1] chosen to be $\zeta = \pi$ such that

$$\hat{C}|\mathrm{K}^0(\mathrm{d}\bar{\mathrm{s}})\rangle = -|\overline{\mathrm{K}}^0(\bar{\mathrm{d}}\mathrm{s})\rangle \quad \text{and} \quad \hat{C}|\overline{\mathrm{K}}^0(\bar{\mathrm{d}}\mathrm{s})\rangle = -|\mathrm{K}^0(\mathrm{d}\bar{\mathrm{s}})\rangle.$$

With this choice, the combined action of $\hat{C}\hat{P}$ on the neutral kaon flavour eigenstates are

$$\hat{C}\hat{P}|\mathrm{K}^0\rangle = +|\overline{\mathrm{K}}^0\rangle \quad \text{and} \quad \hat{C}\hat{P}|\overline{\mathrm{K}}^0\rangle = +|\mathrm{K}^0\rangle.$$

Consequently, the orthogonal linear combinations

$$\mathrm{K}_1 = \tfrac{1}{\sqrt{2}}(\mathrm{K}^0 + \overline{\mathrm{K}}^0) \quad \text{and} \quad \mathrm{K}_2 = \tfrac{1}{\sqrt{2}}(\mathrm{K}^0 - \overline{\mathrm{K}}^0), \tag{14.10}$$

are CP eigenstates with

$$\hat{C}\hat{P}|\mathrm{K}_1\rangle = +|\mathrm{K}_1\rangle \quad \text{and} \quad \hat{C}\hat{P}|\mathrm{K}_2\rangle = -|\mathrm{K}_2\rangle.$$

If CP were conserved in the weak interaction, these states would correspond to the physical K_S and K_L particles. In practice, CP is observed to be violated but at a relatively low level, and to a reasonable approximation it is found that

$$|\mathrm{K}_S\rangle \approx |\mathrm{K}_1\rangle \quad \text{and} \quad |\mathrm{K}_L\rangle \approx |\mathrm{K}_2\rangle.$$

14.4.1 Kaon decays to pions

Neutral kaons propagate as the physical particles K_S and K_L, which have well-defined masses and lifetimes. The K_S and K_L mainly decay to hadronic final states of either two/three pions or to semi-leptonic final states with electrons or muons. For the hadronic decays, the K_S decays mostly to $\pi\pi$ final states, whereas the main hadronic decays of the K_L are to $\pi\pi\pi$ final states,

$$\Gamma(\mathrm{K}_S \to \pi\pi) \gg \Gamma(\mathrm{K}_S \to \pi\pi\pi) \quad \text{and} \quad \Gamma(\mathrm{K}_L \to \pi\pi\pi) \gg \Gamma(\mathrm{K}_L \to \pi\pi).$$

The differences in the lifetimes of the K_S and K_L can be attributed to the different hadronic decay modes that are a consequence of the (near) conservation of CP in kaon decays, as discussed below

First consider the decays to two pions. The two pions can be produced with relative orbital angular momentum ℓ, as indicated in Figure 14.8a. Because kaons and pions both have $J^P = 0^-$, the pions produced in the decay $\mathrm{K} \to \pi^0\pi^0$ must be in an $\ell = 0$ state in order to conserve angular momentum. The overall parity of the $\pi^0\pi^0$ system, which is given by the symmetry of the spatial wavefunction and the intrinsic parity of the pion, is therefore

$$P(\pi^0\pi^0) = (-1)^\ell P(\pi^0)P(\pi^0) = (+1) \times (-1) \times (-1) = +1.$$

[1] Sometimes, the convention $\zeta = 0$ is used, leading to a different definition of the K_1 and K_2 in terms of the flavour eigenstates. However, provided this weak phase is treated consistently, there are no physical consequences in the choice.

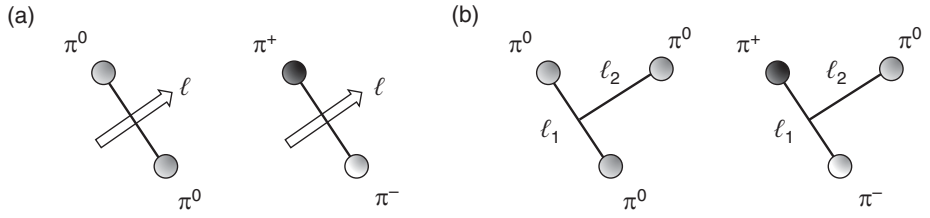

Fig. 14.8 Angular momentum in the two- and three-pion systems.

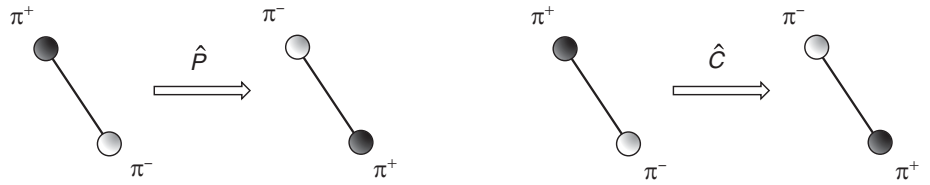

Fig. 14.9 The effect of the parity and charge conjugation operations on the $\pi^+\pi^-$ system in an $\ell = 0$ angular momentum state.

The flavour wavefunction of the π^0 is

$$|\pi^0\rangle = \tfrac{1}{\sqrt{2}}(u\bar{u} - d\bar{d}),$$

and consequently the π^0 is an eigenstate of $\hat{C}$ with eigenvalue +1. Therefore

$$C(\pi^0\pi^0) = C(\pi^0)C(\pi^0) = +1,$$

and since $P(\pi^0\pi^0) = +1$, the $\pi^0\pi^0$ system must be produced in a CP-even state,

$$CP(\pi^0\pi^0) = +1.$$

The angular momentum arguments given above apply equally to the $\pi^+\pi^-$ system, and therefore $P(\pi^+\pi^-) = +1$. The effect of the parity operation on the $\pi^+\pi^-$ system is to swap the positions of the two particles, with no change in sign. Because the charge conjugation operation turns a π^+ into a π^- and vice versa, the effect of the charge conjugation on the $\pi^+\pi^-$ system is also to swap the positions of the particles, with no change in sign. Hence, here the parity and charge conjugation operations have the same effect, as shown in Figure 14.9, and thus $C(\pi^+\pi^-) = P(\pi^+\pi^-) = +1$. Therefore, the decay of a neutral kaon into two pions always produces a CP-even final state,

$$CP(\pi^0\pi^0) = +1 \quad \text{and} \quad CP(\pi^+\pi^-) = +1.$$

If CP is conserved in kaon decay (which it is to a very good approximation), the decay $K \to \pi\pi$ can only occur if the neutral kaon state has CP = +1.

The corresponding arguments for the decays $K \to \pi^0\pi^0\pi^0$ and $K \to \pi^+\pi^-\pi^0$ are slightly more involved. Here, the orbital angular momentum has to be decomposed into two components; the relative angular momentum of the first two particles, $\mathbf{L}_1$,

and the relative angular momentum of the third with respect to the centre of mass of the first two, $\mathbf{L}_2$, as indicated in Figure 14.8b. Because both kaons and pions are spin-0 particles, the total orbital angular momentum in the decay $\mathrm{K} \to \pi\pi\pi$ must be zero, $\mathbf{L} = \mathbf{L}_1 + \mathbf{L}_2 = 0$. This only can be the case if $\ell_1 = \ell_2 = \ell$. The overall parity of the final state in a $\mathrm{K} \to \pi\pi\pi$ decay is therefore

$$P(\pi\pi\pi) = (-1)^{\ell_1}(-1)^{\ell_2}(P(\pi))^3 = (-1)^{2\ell}(-1)^3 = -1.$$

For the $\pi^0\pi^0\pi^0$ final state, the effect of the charge conjugation operator is

$$C(\pi^0\pi^0\pi^0) = C(\pi^0)C(\pi^0)C(\pi^0) = (+1)^3 = +1,$$

and therefore $CP(\pi^0\pi^0\pi^0) = -1$. The effect of the charge conjugation operator on the $\pi^+\pi^-\pi^0$ system follows from the arguments given previously,

$$C(\pi^+\pi^-\pi^0) = C(\pi^+\pi^-)C(\pi^0) = +C(\pi^+\pi^-) = P(\pi^+\pi^-) = (-1)^{\ell_1},$$

where again the effect of $\hat{C}(\pi^+\pi^-)$ is the same as that of $\hat{P}(\pi^+\pi^-)$. Because $m(\mathrm{K}) - 3m(\pi) \approx 80\,\mathrm{MeV}$, the kinetic energy of the three-pion system is relatively small, and the decays where $\ell_1 = \ell_2 > 0$ are suppressed to the point where the contribution is negligible. For this reason ℓ_1 can be taken to be zero and thus

$$CP(\pi^0\pi^0\pi^0) = -1 \quad \text{and} \quad CP(\pi^+\pi^-\pi^0) = -1.$$

Therefore, the $\mathrm{K} \to \pi\pi\pi$ decay modes of neutral kaons always result in a CP-odd final state.

If CP were conserved in the decays of neutral kaons, the hadronic decays of the CP-eigenstates $|\mathrm{K}_1\rangle$ and $|\mathrm{K}_2\rangle$ would be exclusively $\mathrm{K}_1 \to \pi\pi$ and $\mathrm{K}_2 \to \pi\pi\pi$. Because the phase space available for decays to two and three pions is very different, $m(\mathrm{K}) - 2m(\pi) \approx 220\,\mathrm{MeV}$ compared to $m(\mathrm{K}) - 3m(\pi) \approx 80\,\mathrm{MeV}$, the decay rate to two pions is much larger than that to three pions. Hence, the short-lived K_S, which decays mostly to two pions, can be identified as being a close approximation to the CP-even state

$$\mathrm{K}_S \approx \mathrm{K}_1 = \tfrac{1}{\sqrt{2}}(\mathrm{K}^0 + \overline{\mathrm{K}}^0), \tag{14.11}$$

and the longer lived K_L as

$$\mathrm{K}_L \approx \mathrm{K}_2 = \tfrac{1}{\sqrt{2}}(\mathrm{K}^0 - \overline{\mathrm{K}}^0). \tag{14.12}$$

If CP were *exactly* conserved in the weak interaction, then $\mathrm{K}_S \equiv \mathrm{K}_1$ and $\mathrm{K}_L \equiv \mathrm{K}_2$.

CP violation in hadronic kaon decays

The decays of neutral kaons have been extensively studied using kaon beams produced from hadronic interactions. If a neutral kaon is produced in the strong

interaction $\mathrm{p\bar{p}} \rightarrow \mathrm{K^-\pi^+K^0}$, at the time of production, the kaon is the flavour eigenstate,

$$|\mathrm{K}(0)\rangle = |\mathrm{K}^0\rangle.$$

In the absence of CP violation, where $\mathrm{K}_S \equiv \mathrm{K}_1$ and $\mathrm{K}_L \equiv \mathrm{K}_2$, the $|\mathrm{K}^0\rangle$ flavour state can be written in terms of the CP eigenstates using (14.11) and (14.12),

$$|\mathrm{K}(0)\rangle = |\mathrm{K}^0\rangle = \tfrac{1}{\sqrt{2}}[\,|\mathrm{K}_1\rangle + |\mathrm{K}_2\rangle] = \tfrac{1}{\sqrt{2}}[\,|\mathrm{K}_S\rangle + |\mathrm{K}_L\rangle]. \tag{14.13}$$

The subsequent time evolution is described in terms of the K_S and K_L, which are the observed physical neutral kaons with well-defined masses and lifetimes. In the rest frame of the kaon, the time-evolution of the K_S and K_L states are given by

$$|\mathrm{K}_S(t)\rangle = |\mathrm{K}_S\rangle \exp[-im_S t - \Gamma_S t/2], \tag{14.14}$$

$$|\mathrm{K}_L(t)\rangle = |\mathrm{K}_L\rangle \exp[-im_L t - \Gamma_L t/2], \tag{14.15}$$

where the $\exp[-\Gamma t/2]$ terms ensure that the probability densities decay exponentially. For example

$$\langle K_S(t)|K_S(t)\rangle \propto e^{-\Gamma_S t} = e^{-t/\tau_S}.$$

Hence the time evolution of the state of (14.13) is

$$|\mathrm{K}(t)\rangle = \tfrac{1}{\sqrt{2}}\left[|\mathrm{K}_S\rangle e^{-(im_S+\Gamma_S/2)t} + |\mathrm{K}_L\rangle e^{-(im_L+\Gamma_L/2)t}\right],$$

which can be written as

$$|\mathrm{K}(t)\rangle = \tfrac{1}{\sqrt{2}}\left[\theta_S(t)|\mathrm{K}_S\rangle + \theta_L(t)\mathrm{K}_L\right], \tag{14.16}$$

with

$$\theta_S(t) = \exp[-(im_S + \Gamma_S/2)\,t] \quad \text{and} \quad \theta_L(t) = \exp[-(im_L + \Gamma_L/2)\,t]. \tag{14.17}$$

The decay rate to the CP-even two-pion final state is proportional to the K_1 component of the wavefunction, which in the limit where CP is conserved is equivalent to the K_S component. Therefore, if CP is conserved, the decay rate to two pions from a beam that was initially in a pure $|\mathrm{K}^0\rangle$ state is

$$\Gamma(K^0_{t=0} \rightarrow \pi\pi) \propto |\langle K_S|\mathrm{K}(t)\rangle|^2 \propto |\theta_S(t)|^2 = e^{-\Gamma_S t} = e^{-t/\tau_S},$$

and similarly

$$\Gamma(K^0_{t=0} \rightarrow \pi\pi\pi) \propto |\langle K_L|\psi(t)\rangle|^2 \propto e^{-t/\tau_L}.$$

If a kaon beam, which originally consisted of $\mathrm{K}^0(\mathrm{d\bar{s}})$, propagates over a large distance ($L \gg c\tau_S$), the K_S component will decay away leaving a pure K_L beam, as indicated in Figure 14.10. The same would be true for an initial $\overline{\mathrm{K}}^0$ beam.

If CP were conserved in the weak interactions of quarks, the K_L would correspond exactly to the CP-odd K_2 state and at large distances from the production

Table 14.1 The main decay modes of the K_S and K_L.

K_S Decays	BR	K_L Decays	BR
$K_S \to \pi^+\pi^-$	69.2%	$K_L \to \pi^+\pi^-$	0.20%
$K_S \to \pi^0\pi^0$	30.7%	$K_L \to \pi^0\pi^0$	0.09%
$K_S \to \pi^+\pi^-\pi^0$	$\sim 3 \times 10^{-5}$%	$K_L \to \pi^+\pi^-\pi^0$	12.5%
$K_S \to \pi^0\pi^0\pi^0$	–	$K_L \to \pi^0\pi^0\pi^0$	19.5%
$K_S \to \pi^-e^+\nu_e$	0.03%	$K_L \to \pi^-e^+\nu_e$	20.3%
$K_S \to \pi^+e^-\overline{\nu}_e$	0.03%	$K_L \to \pi^+e^-\overline{\nu}_e$	20.3%
$K_S \to \pi^-\mu^+\nu_\mu$	0.02%	$K_L \to \pi^-\mu^+\nu_\mu$	13.5%
$K_S \to \pi^+\mu^-\overline{\nu}_\mu$	0.02%	$K_L \to \pi^+\mu^-\overline{\nu}_\mu$	13.5%

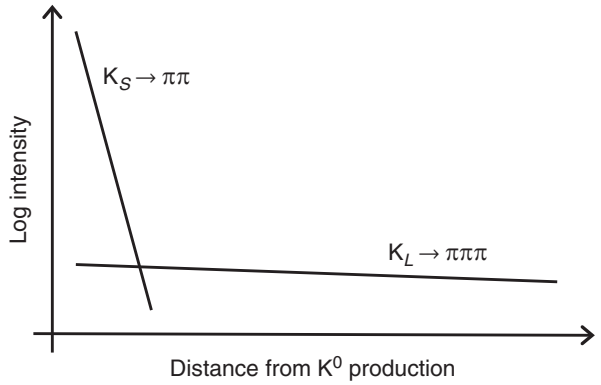

Fig. 14.10 Expected decay rates to pions from an initially pure K^0 beam, assuming no CP violation.

of a kaon beam, the hadronic decays to two pions would never be detected. The first experimental evidence for CP violation was the observation of 45 $K_L \to \pi^+\pi^-$ decays out of a total of 22 700 K_L decays at a large distance from the production of the neutral kaon beam; see Christenson *et al.* (1964). This provided the first direct evidence for CP violation in the neutral kaon system, albeit only at the level of 0.2%, for which Cronin and Fitch were awarded the Nobel prize.

The branching ratios for the main decay modes of the K_S and K_L are listed in Table 14.1, including the relatively rare CP violating hadronic decays. The smallness of the semi-leptonic *branching ratios* of the K_S compared to the K_L, reflects the relatively large $K_S \to \pi\pi$ decay rate; the semi-leptonic partial decay *rates* of the K_S and K_L are almost identical (see Section 14.5.4).

14.4.2 The origin of CP violation

There are two main ways of introducing CP violation into the neutral kaon system. If CP is violated in the $K^0 \leftrightarrow \overline{K}^0$ mixing process (see Section 14.4.3), then the

K_S and K_L will not correspond to the CP eigenstates, K_1 and K_2. Given that the observed level of CP violation is relatively small, the K_S and K_L can be related to the CP eigenstates by the small (complex) parameter ε,

$$|K_S\rangle = \frac{1}{\sqrt{1+|\varepsilon|^2}}\left(|K_1\rangle + \varepsilon|K_2\rangle\right) \quad \text{and} \quad |K_L\rangle = \frac{1}{\sqrt{1+|\varepsilon|^2}}\left(|K_2\rangle + \varepsilon|K_1\rangle\right),$$

such that $K_S \approx K_1$ and $K_L \approx K_2$. In this case, the observed $K_L \to \pi\pi$ decays are accounted for by

$$|K_L\rangle = \frac{1}{\sqrt{1+|\varepsilon|^2}}\left(|K_2\rangle + \varepsilon|K_1\rangle\right) \quad \begin{matrix} \llcorner\!\!\rightarrow \pi\pi \\ \llcorner\!\!\rightarrow \pi\pi\pi \end{matrix}$$

and the relative rate of decays to two pions will be depend on ε.

The second possibility is that CP is violated directly in the decay of a CP eigenstate,

$$|K_L\rangle = |K_2\rangle \quad \begin{matrix} \llcorner\!\!\rightarrow \pi\pi \\ \llcorner\!\!\rightarrow \pi\pi\pi \end{matrix}$$

The relative strength of this direct CP violation in neutral kaon decay is parameterised by ε' with $\Gamma(K_2 \to \pi\pi)/\Gamma(K_2 \to \pi\pi\pi) = \varepsilon'$. Experimentally, it is known that CP is violated in both mixing and directly in the decay. The results of the NA48 experiment at CERN and the KTeV experiment at Fermilab, demonstrate that direct CP violation is a relatively small effect,

$$\Re\mathrm{e}\left(\frac{\varepsilon'}{\varepsilon}\right) = (1.65 \pm 0.26) \times 10^{-3},$$

and ε is already a small parameter. Therefore, the main contribution to CP violation in the neutral kaon system is from $K^0 \leftrightarrow \overline{K}^0$ mixing. The quantum mechanics of mixing in the neutral kaon system is described in detail in the following starred section.

14.4.3 *The quantum mechanics of kaon mixing

To fully understand the physics of the neutral kaon system, it is necessary to consider the quantum mechanical time evolution of the combined K^0–$\overline{K}^0$ system. This is not an easy topic, but the results are important.

In the absence of neutral kaon mixing, the time dependence of the wavefunction of the K^0 would be

$$|K^0(t)\rangle = |K^0\rangle e^{-\Gamma t/2} e^{-imt}, \tag{14.18}$$

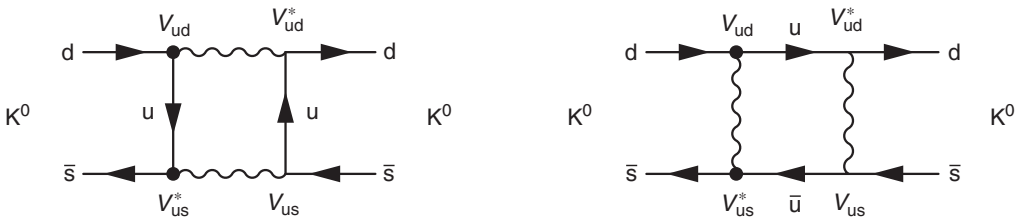

Fig. 14.11 Two box diagrams for $K^0 \leftrightarrow K^0$. There are corresponding diagrams involving all nine combinations of virtual up, charm and top quarks.

where m is the mass of the particle and the term $\Gamma = 1/\tau$ ensures the probability density decays away exponentially. The time-dependent wavefunction of (14.18) clearly satisfies the differential equation

$$i\frac{\partial}{\partial t}|\mathrm{K}^0(t)\rangle = (m - \tfrac{i}{2}\Gamma)|\mathrm{K}^0(t)\rangle,$$

and therefore the *effective* Hamiltonian $\mathcal{H}$ can be identified as

$$\mathcal{H}|\mathrm{K}^0(t)\rangle = (m - \tfrac{i}{2}\Gamma)|\mathrm{K}^0(t)\rangle. \tag{14.19}$$

Because of the inclusion of the exponential decay term in the wavefunction, the effective Hamiltonian is not Hermitian and also the expectation values of operators corresponding to physical observable will not be constant. The mass m in the effective Hamiltonian of (14.19) includes contributions from the masses of the constituent quarks and from the potential energy of the system. The potential energy includes contributions from the strong interaction potential (which is the dominant term), the coulomb interaction and the weak interaction. The interaction terms can be expressed as expectation values of the corresponding interaction Hamiltonians. Therefore the mass of the K^0, when taken in isolation, can be written as

$$m = m_{\mathrm{d}} + m_{\bar{\mathrm{s}}} + \langle \mathrm{K}^0|\hat{H}_{QCD} + \hat{H}_{EM} + \hat{H}_W|\mathrm{K}^0\rangle + \sum_j \frac{\langle \mathrm{K}^0|\hat{H}_W|j\rangle\langle j|\hat{H}_W|\mathrm{K}^0\rangle}{E_j - m_{\mathrm{K}}}. \tag{14.20}$$

The last term in this expression comes from the small second-order $O(G_{\mathrm{F}}^2)$ contribution to the weak interaction potential from the $\mathrm{K}^0 \leftrightarrow \mathrm{K}^0$ box diagrams of Figure 14.11. The decay rate Γ that appears in (14.19) is given by Fermi's golden rule

$$\Gamma = 2\pi \sum_f |\langle f|\hat{H}_W|\mathrm{K}^0\rangle|^2 \rho_f,$$

where the sum is taken over all possible final states, labelled f, and ρ_f is the density of states for that decay mode.

Up to this point, the K^0 has been considered in isolation. However, a K^0 will develop a $\overline{\mathrm{K}}^0$ component through the $\mathrm{K}^0 \leftrightarrow \overline{\mathrm{K}}^0$ mixing diagrams of Figure 14.7.

Consequently, the time evolution of a neutral kaon state must include both K^0 and $\overline{\mathrm{K}}^0$ components,

$$|\mathrm{K}(t)\rangle = a(t)|\mathrm{K}^0\rangle + b(t)|\overline{\mathrm{K}}^0\rangle, \tag{14.21}$$

where the coefficients $a(t)$ and $b(t)$ are the amplitudes and phases of the K^0 and $\overline{\mathrm{K}}^0$ components of the state at a time t. The time evolution of $|\mathrm{K}(t)\rangle$, analogous to (14.19), now has to be written as the coupled equations

$$\begin{pmatrix} M_{11} - \frac{i}{2}\Gamma_{11} & M_{12} - \frac{i}{2}\Gamma_{12} \\ M_{21} - \frac{i}{2}\Gamma_{21} & M_{22} - \frac{i}{2}\Gamma_{22} \end{pmatrix} \begin{pmatrix} a(t)\,|\mathrm{K}^0\rangle \\ b(t)\,|\overline{\mathrm{K}}^0\rangle \end{pmatrix} = i\frac{\partial}{\partial t} \begin{pmatrix} a(t)\,|\mathrm{K}^0\rangle \\ b(t)\,|\overline{\mathrm{K}}^0\rangle \end{pmatrix}, \tag{14.22}$$

and the effective Hamiltonian becomes

$$\mathcal{H} = \mathbf{M} - \tfrac{i}{2}\mathbf{\Gamma} = \begin{pmatrix} M_{11} & M_{12} \\ M_{21} & M_{22} \end{pmatrix} - \tfrac{i}{2}\begin{pmatrix} \Gamma_{11} & \Gamma_{12} \\ \Gamma_{21} & \Gamma_{22} \end{pmatrix}. \tag{14.23}$$

It is important to understand the physical meaning of the terms in (14.23). First consider the decay matrix $\mathbf{\Gamma}$ that accounts for the decay of the state $|\mathrm{K}(t)\rangle$. Here the total decay rate is given by Fermi's golden rule, which to lowest order is

$$\Gamma = 2\pi \sum_f |\langle f|\hat{H}_W|\mathrm{K}(t)\rangle|^2 \rho_f \equiv 2\pi \sum_f \langle \mathrm{K}(t)|\hat{H}_W|f\rangle\langle f|\hat{H}_W|\mathrm{K}(t)\rangle\, \rho_f.$$

By writing $|\mathrm{K}(t)\rangle$ in terms of K^0 and $\overline{\mathrm{K}}^0$, the matrix element squared for the decay to a final state f becomes

$$\begin{aligned} |\langle f|\hat{H}_W|\mathrm{K}(t)\rangle|^2 = {} & |a(t)|^2\, |\langle f|\hat{H}_W|\mathrm{K}^0\rangle|^2 + |b(t)|^2\, |\langle f|\hat{H}_W|\overline{\mathrm{K}}^0\rangle|^2 \\ & + a(t)b(t)^*\, \langle \overline{\mathrm{K}}^0|\hat{H}_W|f\rangle\langle f|\hat{H}_W|\mathrm{K}^0\rangle + a(t)^* b(t)\, \langle \mathrm{K}^0|\hat{H}_W|f\rangle\langle f|\hat{H}_W|\overline{\mathrm{K}}^0\rangle. \end{aligned}$$

The diagonal elements of $\mathbf{\Gamma}$ are therefore given by the decay rates

$$\Gamma_{11} = 2\pi \sum_f |\langle f|\hat{H}_W|\mathrm{K}^0\rangle|^2 \rho_f \quad \text{and} \quad \Gamma_{22} = 2\pi \sum_f |\langle f|\hat{H}_W|\overline{\mathrm{K}}^0\rangle|^2 \rho_f,$$

and are therefore real numbers. The off-diagonal terms of $\mathbf{\Gamma}$ account for the interference between the decays of the K^0 and $\overline{\mathrm{K}}^0$ components of $\mathrm{K}(t)$. Because the two interference terms are the Hermitian conjugates of each other, $\Gamma_{12} = \Gamma_{21}^*$, and the matrix $\mathbf{\Gamma}$ is itself Hermitian.

Now consider the mass matrix $\mathbf{M}$. The diagonal elements are the mass terms for the K^0 and $\overline{\mathrm{K}}^0$ *flavour* eigenstates, with M_{11} given by (14.20) and

$$M_{22} = m_{\mathrm{s}} + m_{\bar{\mathrm{d}}} + \langle \overline{\mathrm{K}}^0|\hat{H}_{QCD} + \hat{H}_{EM} + \hat{H}_W|\overline{\mathrm{K}}^0\rangle + \sum_j \frac{\langle \overline{\mathrm{K}}^0|\hat{H}_W|j\rangle\langle j|\hat{H}_W|\overline{\mathrm{K}}^0\rangle}{E_j - m_{\mathrm{K}}}. \tag{14.24}$$

The off-diagonal terms of $\mathbf{M}$ are due to the $\mathrm{K}^0 \leftrightarrow \overline{\mathrm{K}}^0$ mixing diagrams of Figure 14.7, and can be written

$$M_{12} = M_{21}^* = \sum_j \frac{\langle \overline{\mathrm{K}}^0 | \hat{H}_W | j \rangle \langle j | \hat{H}_W | \mathrm{K}^0 \rangle}{E_j - m_\mathrm{K}}.$$

There is no off-diagonal term of the form $\langle \overline{\mathrm{K}}^0 | \hat{H}_W | \mathrm{K}^0 \rangle$ because there is no Feynman diagram for $\mathrm{K}^0 \leftrightarrow \overline{\mathrm{K}}^0$ mixing involving the exchange of a single W boson. Since $M_{12} = M_{21}^*$ and the diagonal terms of $\mathbf{M}$ are real, the mass matrix is Hermitian. If there were no mixing in the neutral kaon system M_{12}, M_{21}, Γ_{12} and Γ_{21} would all be zero, and the time evolution equation of (14.22) would decouple into two independent equations of the form of (14.19), describing the independent time evolution of the K^0 and $\overline{\mathrm{K}}^0$.

From the required CPT symmetry of the Standard Model, the masses and decay rates of the flavour states K^0 and $\overline{\mathrm{K}}^0$ must be equal, $M_{11} = M_{22} = M$ and $\Gamma_{11} = \Gamma_{22} = \Gamma$. Therefore the effective Hamiltonian of (14.23) can be written as

$$\boldsymbol{\mathcal{H}} = \mathbf{M} - \tfrac{i}{2}\boldsymbol{\Gamma} = \begin{pmatrix} M & M_{12} \\ M_{12}^* & M \end{pmatrix} - \tfrac{i}{2}\begin{pmatrix} \Gamma & \Gamma_{12} \\ \Gamma_{12}^* & \Gamma \end{pmatrix}. \tag{14.25}$$

Because the off-diagonal elements of $\mathbf{M}$ arise from second-order weak interaction box diagrams, they are much smaller than the diagonal elements that include the fermion masses and the strong interaction Hamiltonian. The off-diagonal terms of $\boldsymbol{\Gamma}$, which can be of the same order of magnitude as the diagonal terms, are either positive or negative. Because of the presence of the non-zero off-diagonal terms in $\boldsymbol{\mathcal{H}}$, the flavour eigenstates K^0 and $\overline{\mathrm{K}}^0$ are no longer the eigenstates of the Hamiltonian.

The neutral kaon state of (14.21), evolves in time according to

$$\begin{pmatrix} M - \frac{i}{2}\Gamma & M_{12} - \frac{i}{2}\Gamma_{12} \\ M_{12}^* - \frac{i}{2}\Gamma_{12}^* & M - \frac{i}{2}\Gamma \end{pmatrix} \begin{pmatrix} a(t)\,|\mathrm{K}^0\rangle \\ b(t)\,|\overline{\mathrm{K}}^0\rangle \end{pmatrix} = i\frac{\partial}{\partial t}\begin{pmatrix} a(t)\,|\mathrm{K}^0\rangle \\ b(t)|\overline{\mathrm{K}}^0\rangle \end{pmatrix}. \tag{14.26}$$

The eigenstates of this effective Hamiltonian can be found by transforming (14.26) into the basis where $\boldsymbol{\mathcal{H}}$ is diagonal. The required transformation can be found by first solving the eigenvalue equation

$$\begin{pmatrix} M - \frac{i}{2}\Gamma & M_{12} - \frac{i}{2}\Gamma_{12} \\ M_{12}^* - \frac{i}{2}\Gamma_{12}^* & M - \frac{i}{2}\Gamma \end{pmatrix} \begin{pmatrix} p \\ q \end{pmatrix} = \lambda \begin{pmatrix} p \\ q \end{pmatrix}. \tag{14.27}$$

The non-trivial solutions to (14.27) can be obtained from the characteristic equation, $\det(\boldsymbol{\mathcal{H}} - \lambda I) = 0$, which gives

$$(M - \tfrac{i}{2}\Gamma - \lambda)^2 - (M_{12}^* - \tfrac{i}{2}\Gamma_{12}^*)(M_{12} - \tfrac{i}{2}\Gamma_{12}) = 0.$$

Solving this quadratic equation for λ gives the two eigenvalues

$$\lambda_\pm = M - \tfrac{i}{2}\Gamma \pm \left[(M_{12}^* - \tfrac{i}{2}\Gamma_{12}^*)(M_{12} - \tfrac{i}{2}\Gamma_{12})\right]^{\frac{1}{2}}. \tag{14.28}$$

The corresponding eigenstates, found by substituting these two eigenvalues back into (14.27), have

$$\frac{q}{p} = \pm\xi \equiv \pm\left(\frac{M_{12}^* - \frac{i}{2}\Gamma_{12}^*}{M_{12} - \frac{i}{2}\Gamma_{12}}\right)^{\frac{1}{2}}. \tag{14.29}$$

The normalised eigenstates, here denoted K_+ and K_-, which ultimately will be identified as the K_S and K_L, are therefore

$$\begin{pmatrix} |\mathrm{K}_+\rangle \\ |\mathrm{K}_-\rangle \end{pmatrix} = \frac{1}{\sqrt{1+|\xi|^2}} \begin{pmatrix} 1 & \xi \\ 1 & -\xi \end{pmatrix} \begin{pmatrix} |\mathrm{K}^0\rangle \\ |\overline{\mathrm{K}}^0\rangle \end{pmatrix} = \frac{1}{\sqrt{1+|\xi|^2}} \begin{pmatrix} |\mathrm{K}^0\rangle + \xi|\overline{\mathrm{K}}^0 \\ |\mathrm{K}^0\rangle - \xi|\overline{\mathrm{K}}^0\rangle \end{pmatrix}.$$

Equation (14.26), which has the form $\mathcal{H}\mathbf{K} = i\partial\mathbf{K}/\partial t$, can be written in the diagonal basis using the matrix $\mathbf{S}$ formed from the eigenvectors of $\mathcal{H}$, such that $\mathcal{H}' = \mathbf{S}^{-1}\mathcal{H}\mathbf{S}$ is diagonal,

$$\mathcal{H}' = \mathbf{S}^{-1}\mathcal{H}\mathbf{S} = \begin{pmatrix} \lambda_+ & 0 \\ 0 & \lambda_- \end{pmatrix}.$$

In the diagonal basis (14.26) becomes

$$i\frac{\partial}{\partial t}\begin{pmatrix} |\mathrm{K}_+(t)\rangle \\ |\mathrm{K}_-(t)\rangle \end{pmatrix} = \begin{pmatrix} \lambda_+ & 0 \\ 0 & \lambda_- \end{pmatrix} \begin{pmatrix} |\mathrm{K}_+(t)\rangle \\ |\mathrm{K}_-(t)\rangle \end{pmatrix}. \tag{14.30}$$

Hence the states K_+ and K_- propagate as independent particles and therefore can be identified as the physical mass eigenstates of the neutral kaon system. The time dependences of the K_+ and K_- states are given by the solutions of (14.30),

$$|\mathrm{K}_+(t)\rangle = \frac{1}{\sqrt{1+|\xi|^2}}\left(|\mathrm{K}^0\rangle + \xi|\overline{\mathrm{K}}^0\rangle\right)e^{-i\lambda_+ t}$$
$$|\mathrm{K}_-(t)\rangle = \frac{1}{\sqrt{1+|\xi|^2}}\left(|\mathrm{K}^0\rangle - \xi|\overline{\mathrm{K}}^0\rangle\right)e^{-i\lambda_- t},$$

with the real and imaginary parts of $\lambda_\pm$ determining respectively the masses and decay rates of the two physical states. From (14.28),

$$\lambda_+ - \lambda_- = 2\left[(M_{12}^* - \tfrac{i}{2}\Gamma_{12}^*)(M_{12} - \tfrac{i}{2}\Gamma_{12})\right]^{\frac{1}{2}}, \tag{14.31}$$

and therefore λ_+ and λ_- can be written as

$$\lambda_\pm = M - \tfrac{i}{2}\Gamma \pm \tfrac{1}{2}(\lambda_+ - \lambda_-) = M \pm \mathfrak{Re}\left(\frac{\lambda_+ - \lambda_-}{2}\right) - \tfrac{i}{2}\left(\Gamma \mp \mathfrak{Im}\{\lambda_+ - \lambda_-\}\right).$$

It is not *a priori* clear which of the two eigenvalues, λ_+ and λ_-, is associated with the K_S and which is associated with the K_L, but both can be written in the form

$$\lambda = [M \pm \Delta m/2] - \tfrac{i}{2}\left[\Gamma \pm \Delta\Gamma/2\right],$$

with

$$\Delta m = |\,\mathfrak{Re}\,(\lambda_+ - \lambda_-)| \quad \text{and} \quad \Delta\Gamma = \pm|\Delta\Gamma| = \pm 2|\,\mathfrak{Im}\,(\lambda_+ - \lambda_-)|.$$

Here Δm is *defined* to be positive and the sign of $\Delta\Gamma$ depends on the relative signs of the real and imaginary parts of (14.31), which in turn depends on the off-diagonal terms of the effective Hamiltonian. For the neutral kaon system it turns out that $\Delta\Gamma < 0$, and therefore the heavier state has the smaller decay rate. Consequently, the physical eigenstates of the neutral kaon system consist of a heavier state of mass $M + \Delta m/2$ that can be identified as the longer-lived K_L state and a lighter state with a larger decay rate and mass $M - \Delta m/2$ that can be identified as the K_S,

$$\begin{aligned} \lambda_S &= m_S - \tfrac{i}{2}\Gamma_S \quad \text{with} \quad m_S = M - \Delta m/2 \quad \text{and} \quad \Gamma_S = \Gamma + |\Delta\Gamma|/2, \\ \lambda_L &= m_L - \tfrac{i}{2}\Gamma_L \quad \text{with} \quad m_L = M + \Delta m/2 \quad \text{and} \quad \Gamma_L = \Gamma - |\Delta\Gamma|/2. \end{aligned}$$

Because the off-diagonal terms in the effective Hamiltonian arise from the weak interaction alone, $\Delta m \ll M$, and the mass difference between the K_L and K_S is very small.

If the CKM matrix were entirely real, which would imply that $M_{12} = M_{12}^*$ and $\Gamma_{12} = \Gamma_{12}^*$, the parameter ξ defined in (14.29) would be unity. In this case, the physical states would be

$$\mathrm{K}_S \equiv \mathrm{K}_1 = \tfrac{1}{\sqrt{2}}\left(\mathrm{K}^0 + \overline{\mathrm{K}}^0\right) \quad \text{and} \quad \mathrm{K}_L \equiv \mathrm{K}_2 = \tfrac{1}{\sqrt{2}}\left(\mathrm{K}^0 - \overline{\mathrm{K}}^0\right). \tag{14.32}$$

Hence, *if* the CKM matrix were entirely real, in which case the weak interactions of quarks would conserve CP, the physical states of the neutral kaon system would be the CP eigenstates, K_1 and K_2. In practice, CP violation is observed in the neutral kaon system, albeit at a very low level and therefore $\xi \neq 1$.

Because CP-violating effects are observed to be relatively small, it is convenient to rewrite ξ in terms of the (small) complex parameter ε defined by

$$\xi = \frac{1-\varepsilon}{1+\varepsilon},$$

such that the physical K_S and K_L states are

$$|\mathrm{K}_S(t)\rangle = \frac{1}{\sqrt{2(1+|\varepsilon|^2)}}\left[(1+\varepsilon)|\mathrm{K}^0\rangle + (1-\varepsilon)|\overline{\mathrm{K}}^0\rangle\right] e^{-i\lambda_S t}, \tag{14.33}$$

$$|\mathrm{K}_L(t)\rangle = \frac{1}{\sqrt{2(1+|\varepsilon|^2)}}\left[(1+\varepsilon)|\mathrm{K}^0\rangle - (1-\varepsilon)|\overline{\mathrm{K}}^0\rangle\right] e^{-i\lambda_L t}. \tag{14.34}$$

Using (14.10), the physical states also can be expressed in terms of the CP eigenstates K_1 and K_2,

$$|\mathrm{K}_S(t)\rangle = \frac{1}{\sqrt{1+|\varepsilon|^2}}\left[|\mathrm{K}_1\rangle + \varepsilon|\mathrm{K}_2\rangle\right] e^{-i\lambda_S t}, \tag{14.35}$$

$$|\mathrm{K}_L(t)\rangle = \frac{1}{\sqrt{1+|\varepsilon|^2}}\left[|\mathrm{K}_2\rangle + \varepsilon|\mathrm{K}_1\rangle\right] e^{-i\lambda_L t}. \tag{14.36}$$

14.5 Strangeness oscillations

The previous chapter described how neutrino oscillations arise because neutrinos are created and interact as weak eigenstates but propagate as mass eigenstates. A similar phenomenon occurs in the neutral kaon system. The physical mass eigenstates are the K_S and K_L. However, the hadronic decays to $\pi\pi$ or $\pi\pi\pi$ have to be described in terms of the CP eigenstates and the semi-leptonic decays of the K_S and K_L have to be described in terms of the flavour eigenstates, K^0 and $\overline{\mathrm{K}}^0$. For example, Figure 14.12 shows the Feynman diagrams for the allowed decays $\mathrm{K}^0 \to \pi^-\mathrm{e}^+\nu_\mathrm{e}$ and $\overline{\mathrm{K}}^0 \to \pi^+\mathrm{e}^-\overline{\nu}_\mathrm{e}$. There are no corresponding Feynman diagrams for $\mathrm{K}^0 \to \pi^+\mathrm{e}^-\overline{\nu}_\mathrm{e}$ and $\overline{\mathrm{K}}^0 \to \pi^-\mathrm{e}^+\nu_\mathrm{e}$ because the charge of the lepton depends on whether $\mathrm{s} \to \mathrm{u}$ or $\overline{\mathrm{s}} \to \overline{\mathrm{u}}$ decay is involved:

$$\begin{aligned} &\mathrm{K}^0 \to \pi^-\mathrm{e}^+\nu_\mathrm{e} \quad \text{and} \quad \overline{\mathrm{K}}^0 \to \pi^+\mathrm{e}^-\overline{\nu}_\mathrm{e}, \\ &\mathrm{K}^0 \not\to \pi^+\mathrm{e}^-\overline{\nu}_\mathrm{e} \quad \text{and} \quad \overline{\mathrm{K}}^0 \not\to \pi^-\mathrm{e}^+\nu_\mathrm{e}. \end{aligned}$$

Hence neutral kaons are produced and decay as flavour and/or CP eigenstates, but propagate as the K_S and K_L mass eigenstates. The result is the phenomenon of strangeness oscillations, which occurs regardless of whether CP is violated or not.

14.5.1 Strangeness oscillations neglecting CP violation

Consider a neutral kaon that is produced as the flavour eigenstate K^0. The time evolution of the wavefunction is described in terms of the K_S and K_L mass eigenstates,

$$|\mathrm{K}(t)\rangle = \tfrac{1}{\sqrt{2}}\left[\,\theta_S(t)|\mathrm{K}_S\rangle + \theta_L(t)|\mathrm{K}_L\rangle\right], \tag{14.37}$$

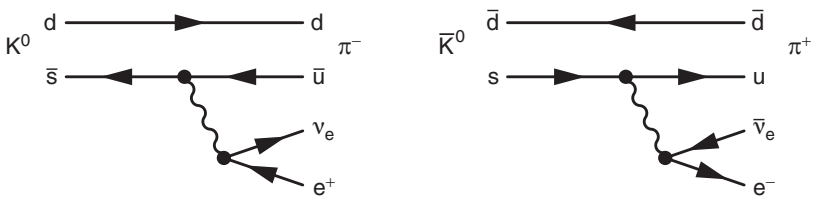

Fig. 14.12 The Feynman diagrams for $\mathrm{K}^0 \to \pi^-\mathrm{e}^+\nu_\mathrm{e}$ and $\overline{\mathrm{K}}^0 \to \pi^+\mathrm{e}^-\overline{\nu}_\mathrm{e}$.

where $\theta_S(t)$ and $\theta_L(t)$ are given by (14.17). In the limit where CP violation is neglected, in which case $\mathrm{K}_S = \mathrm{K}_1$ and $\mathrm{K}_L = \mathrm{K}_2$, this can be expressed in terms of the flavour eigenstates using (14.11) and (14.12),

$$\begin{aligned}|\mathrm{K}(t)\rangle &\approx \tfrac{1}{2}\left(\theta_S\left[|\mathrm{K}^0\rangle + |\overline{\mathrm{K}}^0\rangle\right] + \theta_L\left[|\mathrm{K}^0\rangle - |\overline{\mathrm{K}}^0\rangle\right]\right)\\ &= \tfrac{1}{2}\left(\theta_S + \theta_L\right)|\mathrm{K}^0\rangle + \tfrac{1}{2}\left(\theta_S - \theta_L\right)|\overline{\mathrm{K}}^0\rangle.\end{aligned}$$

Because the masses of the K_S and K_L are slightly different, the oscillatory parts of $\theta_S(t)$ and $\theta_L(t)$ differ, and the initially pure K^0 beam will develop a $\overline{\mathrm{K}}^0$ component. The corresponding strangeness oscillation probabilities are

$$P(\mathrm{K}^0_{t=0} \to \mathrm{K}^0) = |\langle \mathrm{K}^0|\mathrm{K}(t)\rangle|^2 = \tfrac{1}{4}|\theta_S + \theta_L|^2, \tag{14.38}$$

$$P(\mathrm{K}^0_{t=0} \to \overline{\mathrm{K}}^0) = |\langle \overline{\mathrm{K}}^0|\mathrm{K}(t)\rangle|^2 = \tfrac{1}{4}|\theta_S - \theta_L|^2. \tag{14.39}$$

This can be simplified by using the identity, $|\theta_S \pm \theta_L|^2 = |\theta_S|^2 + |\theta_L|^2 \pm 2\,\Re\mathrm{e}(\theta_S\theta_L^*)$,

$$\begin{aligned}|\theta_S(t) \pm \theta_L(t)|^2 &= e^{-\Gamma_S t} + e^{-\Gamma_L t} \pm 2\,\Re\mathrm{e}\left\{e^{-im_S t}e^{-\frac{1}{2}\Gamma_S t}\cdot e^{+im_L t}e^{-\frac{1}{2}\Gamma_L t}\right\}\\ &= e^{-\Gamma_S t} + e^{-\Gamma_L t} \pm 2e^{-\frac{1}{2}(\Gamma_S+\Gamma_L)t}\,\Re\mathrm{e}\left\{e^{i(m_L-m_S)t}\right\}\\ &= e^{-\Gamma_S t} + e^{-\Gamma_L t} \pm 2e^{-\frac{1}{2}(\Gamma_S+\Gamma_L)t}\cos(\Delta m\, t),\end{aligned}$$

where $\Delta m = m(\mathrm{K}_L) - m(\mathrm{K}_S)$. Substituting the above expression into (14.38) and (14.39) leads to

$$P(\mathrm{K}^0_{t=0} \to \mathrm{K}^0) = \tfrac{1}{4}\left[e^{-\Gamma_S t} + e^{-\Gamma_L t} + 2e^{-\frac{1}{2}(\Gamma_S+\Gamma_L)t}\cos(\Delta m\, t)\right], \tag{14.40}$$

$$P(\mathrm{K}^0_{t=0} \to \overline{\mathrm{K}}^0) = \tfrac{1}{4}\left[e^{-\Gamma_S t} + e^{-\Gamma_L t} - 2e^{-\frac{1}{2}(\Gamma_S+\Gamma_L)t}\cos(\Delta m\, t)\right]. \tag{14.41}$$

The above equations are reminiscent of the two-flavour neutrino oscillation probabilities, except here the amplitudes of the oscillations decay at a rate given by the arithmetic mean of the K_S and K_L decay rates.

Using the measured value of Δm (see Section 14.5.2), the corresponding period of the strangeness oscillations is

$$T_{osc} = \frac{2\pi\hbar}{\Delta m} \approx 1.2 \times 10^{-9}\,\mathrm{s},$$

which turns out to be greater than the K_S lifetime, $\tau(\mathrm{K}_S) = 0.9 \times 10^{-10}$ s. Consequently, after one oscillation period, the K_S and oscillatory components of (14.40) and (14.41) will have decayed away leaving an essentially pure K_L beam. The resulting oscillation probabilities are plotted in Figure 14.13. Because of the relatively rapid decay of the K_S component, the oscillatory structure is not particularly pronounced. Nevertheless, the observation of strangeness oscillations provides a method to measure Δm.

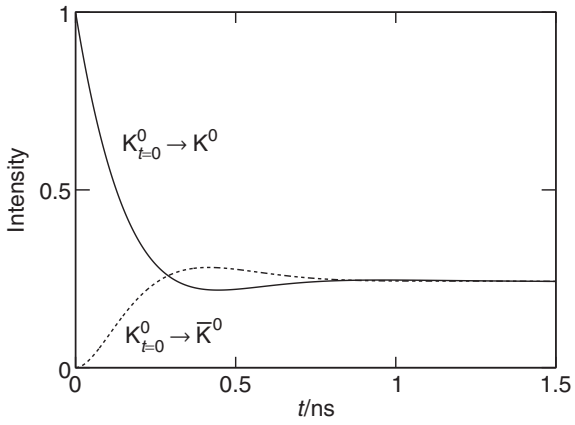

Fig. 14.13 The effect of strangeness oscillations, showing the relative K^0 and $\overline{K}^0$ components in a beam that was produced as a K^0 plotted against time.

14.5.2 The CPLEAR experiment

Strangeness oscillations can be studied by using the semi-leptonic decays of the neutral kaon system. Because the decays $K^0 \to \pi^+\ell^-\overline{\nu}_\ell$ and $\overline{K}^0 \to \pi^-\ell^+\nu_\ell$ ($\ell = e, \mu$) do not occur, the charge of the observed lepton in the semi-leptonic decays $K^0 \to \pi^-\ell^+\nu_\ell$ and $\overline{K}^0 \to \pi^+\ell^-\overline{\nu}_\ell$ uniquely tags the flavour eigenstate from which the decay originated.

The CPLEAR experiment, which operated from 1990 to 1996 at CERN, studied strangeness oscillations and CP violation in the neutral kaon system. It used a low-energy antiproton beam to produce kaons through the strong interaction processes

$$\overline{p}p \to K^-\pi^+K^0 \quad \text{and} \quad \overline{p}p \to K^+\pi^-\overline{K}^0.$$

The energy of the beam was sufficiently low that the particles were produced almost at rest. This enabled the production and decay to be observed in the same detector. The charge of the observed $K^\pm\pi^\mp$ identifies the flavour state of the neutral kaon produced in the $\overline{p}p$ interaction as being either a $\overline{K}^0$ or K^0. The neutral kaon then propagates at a low velocity as the linear combinations of the K_S and K_L with the time dependence given by (14.37). The charge of the observed lepton in the semi-leptonic decay then identifies the decay as coming from either a K^0 or $\overline{K}^0$, thus tagging the flavour component of the wavefunction at the time of decay. For example, Figure 14.14 shows an event in the CPLEAR detector where a K^0 is produced at the origin along with a $K^-\pi^+$, where the K^- is distinguished from a π^- by the absence of an associated signal in the Čerenkov detectors used for particle identification, see Section 1.2.1. The neutral kaon state subsequently decays as a $\overline{K}^0$, identified by its leptonic decay $\overline{K}^0 \to \pi^+e^-\overline{\nu}_e$. The relative rates of decays

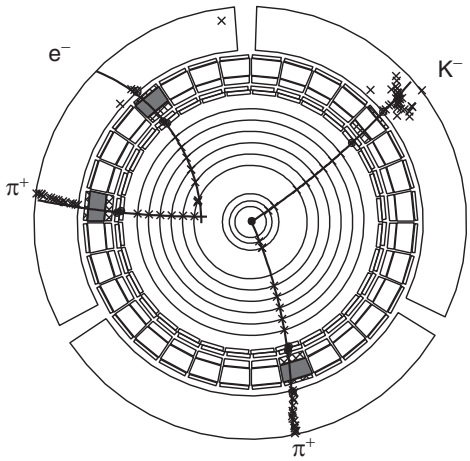

Fig. 14.14 An event in the CPLEAR detector where a K^0 is produced in $\bar{p}p \to K^-\pi^+K^0$ and decays as $\overline{K}^0 \to \pi^+e^-\overline{\nu}_e$. The grey boxes indicate signals from relativistic particles in the Čerenkov detectors. Courtesy of the CPLEAR Collaboration.

from K^0 and $\overline{K}^0$ as a function of the distance between the production point and the decay vertex, provides a direct measure of the relative K^0 and $\overline{K}^0$ components of the neutral kaon wavefunction as a function of time.

For a kaon initially produced as a K^0, the decay rates to $\pi^-e^+\nu_e$ and $\pi^+e^-\overline{\nu}_e$, denoted R_+ and R_- respectively, are given by (14.40) and (14.41),

$$R_+ \propto P(K^0_{t=0} \to K^0) = N\tfrac{1}{4}\left[e^{-\Gamma_S t} + e^{-\Gamma_L t} + 2e^{-(\Gamma_S+\Gamma_L)t/2}\cos(\Delta m\, t)\right],$$
$$R_- \propto P(K^0_{t=0} \to \overline{K}^0) = N\tfrac{1}{4}\left[e^{-\Gamma_S t} + e^{-\Gamma_L t} - 2e^{-(\Gamma_S+\Gamma_L)t/2}\cos(\Delta m\, t)\right],$$

where N is an overall normalisation factor related to the number of $p\overline{p}$ interactions. The corresponding expressions for the decays of neutral kaons that were produced as the $\overline{K}^0$ flavour state are

$$\overline{R}_+ \propto P(\overline{K}^0_{t=0} \to K^0) = N\tfrac{1}{4}\left[e^{-\Gamma_S t} + e^{-\Gamma_L t} - 2e^{-(\Gamma_S+\Gamma_L)t/2}\cos(\Delta m\, t)\right],$$
$$\overline{R}_- \propto P(\overline{K}^0_{t=0} \to \overline{K}^0) = N\tfrac{1}{4}\left[e^{-\Gamma_S t} + e^{-\Gamma_L t} + 2e^{-(\Gamma_S+\Gamma_L)t/2}\cos(\Delta m\, t)\right].$$

Because the QCD interaction is charge conjugation symmetric, equal numbers of K^0 and $\overline{K}^0$ are produced in the $\bar{p}p$ strong interaction and the same normalisation factor applies to $R_\pm$ and $\overline{R}_\pm$. The dependence on the overall normalisation can be removed by expressing the experimental measurements in terms of the asymmetry,

$$A_{\Delta m}(t) = \frac{(R_+ + \overline{R}_-) - (R_- + \overline{R}_+)}{(R_+ + \overline{R}_-) + (R_- + \overline{R}_+)},$$

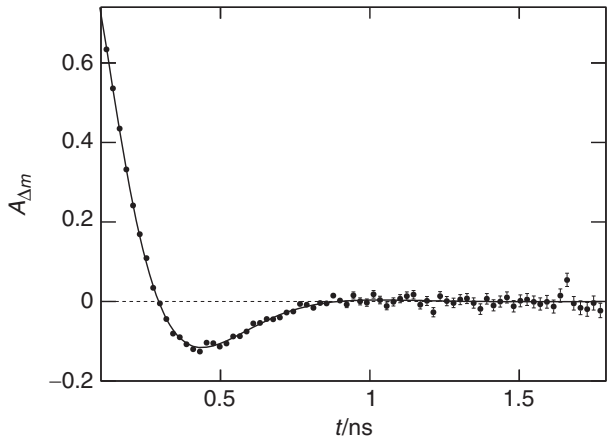

Fig. 14.15 The CPLEAR measurement of $A_{\Delta m}$ as a function of time. The curve shows expression of (14.42) for $\Delta m = 3.485 \times 10^{-15}$ GeV, modified to include the effects of the experimental timing resolution. Adapted from Angelopoulos *et al.* (2001).

which has the advantage that a number of potential systematic biases cancel. This asymmetry can be expressed as a function of time using the above expressions for $R_\pm$ and $\overline{R}_\pm$,

$$A_{\Delta m}(t) = \frac{2e^{-(\Gamma_S+\Gamma_L)t/2}\cos(\Delta m t)}{e^{-\Gamma_S t} + e^{-\Gamma_L t}}. \tag{14.42}$$

The experimental measurements of $A_{\Delta m}(t)$ from the CPLEAR experiment are shown in Figure 14.15. The effects of strangeness oscillations are clearly seen and the position of the minimum provides a precise measurement of Δm. The combined results from several experiments, including the CPLEAR experiment and the KTeV experiment at Fermilab, give

$$\Delta m = m(\mathrm{K}_L) - m(\mathrm{K}_S) = (3.483 \pm 0.006) \times 10^{-15}\ \mathrm{GeV}.$$

14.5.3 CP violation in the neutral kaon system

CP violation in the neutral kaon system has been studied by a number of experiments, including CPLEAR. If there is CP violation in $\mathrm{K}^0 \leftrightarrow \overline{\mathrm{K}}^0$ mixing process, the physical states of the neutral hadron system are

$$|\mathrm{K}_S\rangle = \frac{1}{\sqrt{1+|\varepsilon|^2}}\left(|\mathrm{K}_1\rangle + \varepsilon|\mathrm{K}_2\rangle\right) \quad \text{and} \quad |\mathrm{K}_L\rangle = \frac{1}{\sqrt{1+|\varepsilon|^2}}\left(|\mathrm{K}_2\rangle + \varepsilon|\mathrm{K}_1\rangle\right), \tag{14.43}$$

which can be expressed in terms of the flavour eigenstates as

$$|\mathrm{K}_S\rangle = \frac{1}{\sqrt{2(1+|\varepsilon|^2)}}\left[(1+\varepsilon)|\mathrm{K}^0\rangle + (1-\varepsilon)|\overline{\mathrm{K}}^0\rangle\right],$$
$$|\mathrm{K}_L\rangle = \frac{1}{\sqrt{2(1+|\varepsilon|^2)}}\left[(1+\varepsilon)|\mathrm{K}^0\rangle - (1-\varepsilon)|\overline{\mathrm{K}}^0\rangle\right].$$

The corresponding expressions for the flavour eigenstates in terms of the physical K_S and K_L are

$$|\mathrm{K}^0\rangle = \tfrac{1}{1+\varepsilon}\sqrt{\tfrac{1+|\varepsilon|^2}{2}}\,(|\mathrm{K}_S\rangle + |\mathrm{K}_L\rangle) \quad \text{and} \quad |\overline{\mathrm{K}}^0\rangle = \tfrac{1}{1-\varepsilon}\sqrt{\tfrac{1+|\varepsilon|^2}{2}}\,(|\mathrm{K}_S\rangle - |\mathrm{K}_L\rangle).$$

Therefore, accounting for the possibility of CP violation in neutral kaon mixing, a neutral kaon state that was produced as a K^0 evolves as

$$|\mathrm{K}(t)\rangle = \frac{1}{1+\varepsilon}\sqrt{\frac{1+|\varepsilon|^2}{2}}\,[\theta_S(t)|\mathrm{K}_S\rangle + \theta_L(t)|\mathrm{K}_L\rangle], \tag{14.44}$$

where as before $\theta_S(t)$ and $\theta_L(t)$ are given by (14.17). Direct CP violation in kaon decay is a relatively small effect ($\varepsilon'/\varepsilon \sim 10^{-3}$) and decays to the $\pi\pi$ final state can be taken to originate almost exclusively from the CP-even K_1 component of the wavefunction. The time evolution of (14.44) can be expressed in terms of the K_1 and K_2 states using (14.43)

$$\begin{aligned}|\mathrm{K}(t)\rangle &= \tfrac{1}{\sqrt{2}}\frac{1}{(1+\varepsilon)}\,[\theta_S(|\mathrm{K}_1\rangle + \varepsilon|\mathrm{K}_2\rangle) + \theta_L(|\mathrm{K}_2\rangle + \varepsilon|\mathrm{K}_1\rangle)]\\ &= \tfrac{1}{\sqrt{2}}\frac{1}{(1+\varepsilon)}\,[(\theta_S + \varepsilon\theta_L)|\mathrm{K}_1\rangle + (\theta_L + \varepsilon\theta_S)|\mathrm{K}_2\rangle].\end{aligned}$$

The decay rate to two pions is therefore given by

$$\Gamma(\mathrm{K}^0_{t=0} \to \pi\pi) \propto |\langle \mathrm{K}_1|\mathrm{K}(t)\rangle|^2 = \tfrac{1}{2}\left|\frac{1}{1+\varepsilon}\right|^2 |\theta_S + \varepsilon\theta_L|^2. \tag{14.45}$$

Because $|\varepsilon| \ll 1$,

$$\left|\frac{1}{1+\varepsilon}\right|^2 = \frac{1}{(1+\varepsilon^*)(1+\varepsilon)} \approx \frac{1}{1+2\,\Re\mathrm{e}\{\varepsilon\}} \approx 1 - 2\,\Re\mathrm{e}\{\varepsilon\}.$$

The term $|\theta_S + \varepsilon\theta_L|^2$ can be simplified using $|\theta_S \pm \varepsilon\theta_L|^2 = |\theta_S|^2 + |\theta_L|^2 \pm 2\,\Re\mathrm{e}(\theta_S\varepsilon^*\theta_L^*)$ and by writing $\varepsilon = |\varepsilon|e^{i\phi}$,

$$\begin{aligned}|\theta_S + \varepsilon\theta_L|^2 &= \left|e^{-im_S t - \Gamma_S t/2} + |\varepsilon|e^{i\phi}e^{-im_L t - \Gamma_L t/2}\right|^2\\ &= e^{-\Gamma_S t} + |\varepsilon|^2 e^{-\Gamma_L t} + 2|\varepsilon|e^{-(\Gamma_S+\Gamma_L)t/2}\cos(\Delta m\, t - \phi).\end{aligned}$$

Therefore (14.45) can be written as

$$\Gamma(\mathrm{K}^0_{t=0} \to \pi\pi) = \frac{N}{2}\,(1 - 2\,\Re\mathrm{e}\{\varepsilon\})\left[e^{-\Gamma_S t} + |\varepsilon|^2 e^{-\Gamma_L t} + 2|\varepsilon|e^{-(\Gamma_S+\Gamma_L)t/2}\cos(\Delta m\, t - \phi)\right], \tag{14.46}$$

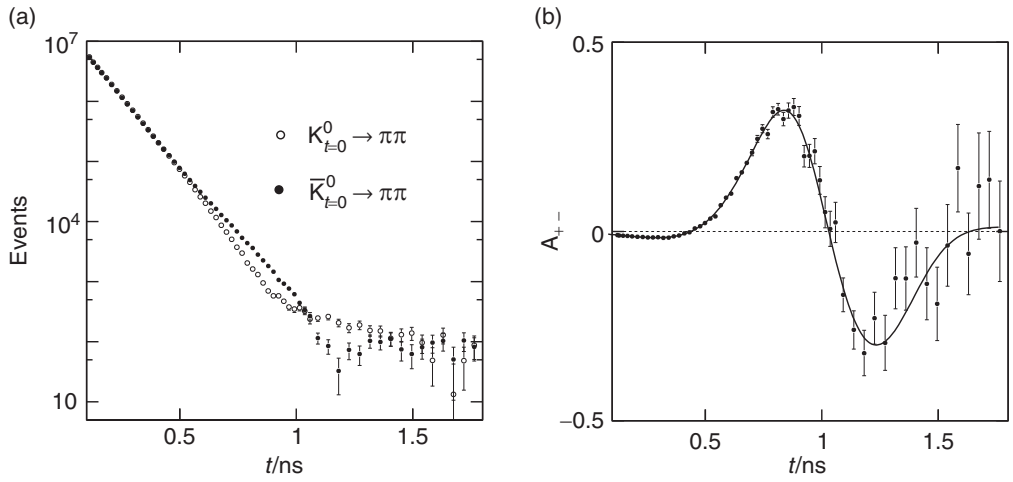

Fig. 14.16 The CPLEAR measurement of A_{+-}. Adapted from Angelopoulos *et al.* (2000).

where N is a normalisation factor. The first term in the square brackets corresponds to the contribution from K_S decays. The second term is the contribution from K_L decays, which is small since $|\varepsilon|^2 \ll 1$. The final term is the interference between the K_S and K_L components of the wavefunction. The corresponding expression for the decay rate to two pions from a state that was initially a $\overline{K}^0$ is

$$\Gamma(\overline{K}^0_{t=0} \to \pi\pi) = \frac{N}{2}(1 + 2\,\Re\mathrm{e}\{\varepsilon\})\left[e^{-\Gamma_S t} + |\varepsilon|^2 e^{-\Gamma_L t} - 2|\varepsilon| e^{-(\Gamma_S+\Gamma_L)t/2}\cos(\Delta m\, t - \phi)\right]. \tag{14.47}$$

Here the interference term has the opposite sign to that of (14.46). For $t \ll \tau_S$ and $t \gg \tau_L$ the expressions of (14.46) and (14.47) are approximately equal, but at intermediate times, the interference term results in a significant difference in the $\pi\pi$ decay rates. Figure 14.16a shows the numbers of $K \to \pi^+\pi^-$ decays observed in the CPLEAR experiment, plotted as a function of the neutral kaon decay time for events that were initially tagged as either a K^0 or $\overline{K}^0$. The difference in the region of $t \sim 1$ ns is the result of this interference term and the magnitude of the difference is proportional to $|\varepsilon|$.

In practice, the experimental measurement of ε at CPLEAR was obtained from the asymmetry A_{+-}, defined as

$$A_{+-} = \frac{\Gamma\left(\overline{K}^0_{t=0} \to \pi^+\pi^-\right) - \Gamma\left(K^0_{t=0} \to \pi^+\pi^-\right)}{\Gamma\left(\overline{K}^0_{t=0} \to \pi^+\pi^-\right) + \Gamma\left(K^0_{t=0} \to \pi^+\pi^-\right)}. \tag{14.48}$$

From (14.46) and (14.47), this can be expressed as

$$A_{+-} = \frac{4\,\Re\mathrm{e}\{\varepsilon\}\left[e^{-\Gamma_S t} + |\varepsilon|^2 e^{-\Gamma_L t}\right] - 4|\varepsilon| e^{-(\Gamma_L+\Gamma_S)t/2}\cos(\Delta m\, t - \phi)}{2\left[e^{-\Gamma_S t} + |\varepsilon|^2 e^{-\Gamma_L t}\right] - 8\,\Re\mathrm{e}\{\varepsilon\}|\varepsilon| e^{-(\Gamma_L+\Gamma_S)t/2}\cos(\Delta m\, t - \phi)}.$$

Since ε is small, the term in the denominator that is proportional to $|\varepsilon|\,\mathfrak{Re}\{\varepsilon\}$ can be neglected at all times, giving

$$\begin{aligned} A_{+-} &\approx 2\,\mathfrak{Re}\{\varepsilon\} - \frac{2|\varepsilon| e^{-(\Gamma_L+\Gamma_S)t/2}\cos(\Delta m\, t - \phi)}{e^{-\Gamma_S t} + |\varepsilon|^2 e^{-\Gamma_L t}} \\ &= 2\,\mathfrak{Re}\{\varepsilon\} - \frac{2|\varepsilon| e^{(\Gamma_S-\Gamma_L)t/2}\cos(\Delta m\, t - \phi)}{1 + |\varepsilon|^2 e^{(\Gamma_S-\Gamma_L)t}}. \end{aligned} \tag{14.49}$$

Hence both the phase and magnitude of ε can be cleanly extracted from the experimental measurement of A_{+-}. Figure 14.16b shows the asymmetry A_{+-} obtained from the CPLEAR data of Figure 14.16a. The measured asymmetry is well described by (14.49) with the measured parameters

$$|\varepsilon| = (2.264 \pm 0.035) \times 10^{-3} \quad \text{and} \quad \phi = (43.19 \pm 0.73)^\circ. \tag{14.50}$$

The non-zero value of $|\varepsilon|$ provides clear evidence for CP violation in the weak interaction. Because ϕ is close to 45°, the real and imaginary parts of ε are roughly the same size, $\mathfrak{Re}\{\varepsilon\} \approx \mathfrak{Im}\{\varepsilon\}$.

14.5.4 CP violation in leptonic decays

We can also observe CP violation in the semi-leptonic decays of the K_L from measurements at a large distance from the production of the $\mathrm{K}^0/\overline{\mathrm{K}}^0$. Since the semi-leptonic decays occur from a particular kaon flavour eigenstate, the relative decay rates can be obtained from the K_L wavefunction expressed in terms of its K^0 and $\overline{\mathrm{K}}^0$ components,

$$|\mathrm{K}_L\rangle = \frac{1}{\sqrt{2(1+|\varepsilon^2|)}}\Big[(1+\varepsilon)|\mathrm{K}^0\rangle - (1-\varepsilon)|\overline{\mathrm{K}}^0\rangle\Big].$$

($|\mathrm{K}^0\rangle \to \pi^-\mathrm{e}^+\nu_\mathrm{e}$; $|\overline{\mathrm{K}}^0\rangle \to \pi^+\mathrm{e}^-\overline{\nu}_\mathrm{e}$)

Hence the decay rates are

$$\begin{aligned} \Gamma(\mathrm{K}_L \to \pi^+\mathrm{e}^-\overline{\nu}_\mathrm{e}) &\propto |\langle\overline{\mathrm{K}}^0|\mathrm{K}_L\rangle|^2 \propto |1-\varepsilon|^2 \approx 1 - 2\,\mathfrak{Re}\,(\varepsilon), \\ \Gamma(\mathrm{K}_L \to \pi^-\mathrm{e}^+\nu_\mathrm{e}) &\propto |\langle\mathrm{K}^0|\mathrm{K}_L\rangle|^2 \propto |1+\varepsilon|^2 \approx 1 + 2\,\mathfrak{Re}\,(\varepsilon). \end{aligned}$$

The experimental measurements are conveniently expressed in terms of the charge asymmetry δ defined as

$$\delta = \frac{\Gamma(\mathrm{K}_L \to \pi^-\mathrm{e}^+\nu_\mathrm{e}) - \Gamma(\mathrm{K}_L \to \pi^+\mathrm{e}^-\overline{\nu}_\mathrm{e})}{\Gamma(\mathrm{K}_L \to \pi^-\mathrm{e}^+\nu_\mathrm{e}) + \Gamma(\mathrm{K}_L \to \pi^+\mathrm{e}^-\overline{\nu}_\mathrm{e})} \approx 2\,\mathfrak{Re}\,(\varepsilon) = 2|\varepsilon|\cos\phi.$$

Experimentally, the number of observed $\mathrm{K}_L \to \pi^-\mathrm{e}^+\nu_\mathrm{e}$ decays is found to be 0.66% larger than the number of $\mathrm{K}_L \to \pi^+\mathrm{e}^-\overline{\nu}_\mathrm{e}$ decays, giving

$$\delta = 0.327 \pm 0.012\%. \tag{14.51}$$

This is consistent with the expectation from the measured values of $|\varepsilon|$ and ϕ given in (14.50), which predict a charge asymmetry of $\delta = 0.33\%$.

Interestingly, the small difference in the $K_L \to \pi^- e^+ \nu_e$ and $K_L \to \pi^- e^- \overline{\nu}_e$ decay rates can be used to provide an unambiguous definition of what we mean by matter as opposed to antimatter, which in principle, could be communicated to aliens in a distant galaxy; the electrons in the atoms in our region of the Universe have the same charge sign as those emitted least often in the decays of the long-lived neutral kaons. Interesting, but perhaps of little practical use.

14.5.5 Interpretation of the neutral kaon data

The size of the mass splitting $\Delta m = m(K_L) - m(K_S)$ and magnitude of the CP violating parameter ε can be related to the elements of CKM matrix and how they enter the matrix elements for $K^0 \leftrightarrow \overline{K}^0$ mixing. In the box diagrams responsible for neutral kaon mixing, shown in Figure 14.17, there are nine possible combinations of u, c and t flavours for the two virtual quarks. The matrix element for each box diagram has the dependence

$$\mathcal{M}_{qq'} \propto V_{qd} V_{qs}^* V_{q's}^* V_{q'd}.$$

For reasons that are explained below, to first order, the value of ε is determined by the matrix elements for box diagrams involving at least one top quark, whereas the dominant contributions to the K_L and K_S mass splitting arises from box diagrams with combinations of virtual up- and charm quarks. A full treatment of these calculations is beyond the scope of this book, but the essential physical concepts can be readily understood.

The mass splitting Δm can be related to the magnitude of the matrix elements for $K^0 \leftrightarrow \overline{K}^0$ mixing. Owing to the smallness of $|V_{td}|$ and $|V_{ts}|$, the diagrams involving the top quark can, to a first approximation, be neglected (see Problem 14.8). Hence the overall matrix element for $K^0 \leftrightarrow \overline{K}^0$ mixing can be written

$$\mathcal{M} \approx \mathcal{M}_{uu} + \mathcal{M}_{uc} + \mathcal{M}_{cu} + \mathcal{M}_{cc}.$$

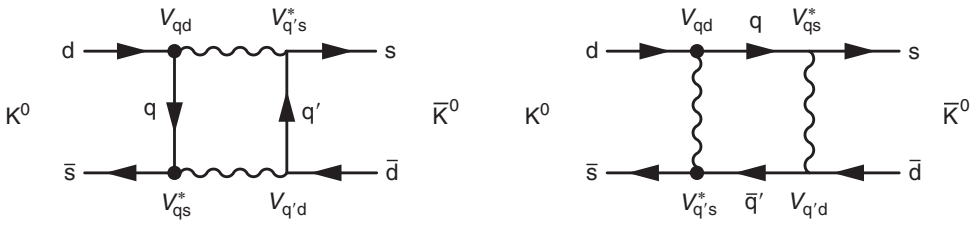

Fig. 14.17 The box diagrams for $K^0 \leftrightarrow \overline{K}^0$ mixing, where the virtual quarks can be any of the nine combinations of $q, q' = \{u, c, t\}$.

The individual matrix elements will be proportional to G_F^2 and will include propagator terms for the two virtual quarks involved and hence

$$\mathcal{M} \sim G_F^2 \left[\frac{V_{ud} V_{us}^* V_{ud} V_{us}^*}{(k^2 - m_u^2)^2} + 2 \frac{V_{ud} V_{us}^* V_{cd} V_{cs}^*}{(k^2 - m_u^2)(k^2 - m_c^2)} + \frac{V_{cd} V_{cs}^* V_{cd} V_{cs}^*}{(k^2 - m_c^2)^2} \right],$$

where k is the four-momentum appearing in the box of virtual particles. Writing $V_{ud} \approx V_{cs} \approx \cos\theta_c$ and $V_{us} \approx -V_{cd} \approx \sin\theta_c$, this can be expressed as

$$\begin{aligned} \mathcal{M} &\sim G_F^2 \left[\frac{\sin^2\theta_c \cos^2\theta_c}{(k^2 - m_u^2)^2} - 2 \frac{\sin^2\theta_c \cos^2\theta_c}{(k^2 - m_u^2)(k^2 - m_c^2)} + \frac{\sin^2\theta_c \cos^2\theta_c}{(k^2 - m_c^2)^2} \right] \\ &\sim G_F^2 \sin^2\theta_c \cos^2\theta_c \frac{(m_c^2 - m_u^2)^2}{(k^2 - m_u^2)^2 (k^2 - m_c^2)^2}. \end{aligned}$$

If the masses of the up- and charm quarks were identical, this contribution to the matrix element for $K^0 \leftrightarrow \overline{K}^0$ mixing would vanish. The evaluation of the matrix element, which involves the integration over the four-momentum k, is non-trivial and the resulting expression for Δm is simply quoted here

$$\Delta m \approx \frac{G_F^2}{3\pi^2} \sin^2\theta_c \cos^2\theta_c f_K^2 m_K \frac{(m_c^2 - m_u^2)^2}{m_c^2}. \tag{14.52}$$

In this expression $f_K \sim 170\,\text{MeV}$ is the kaon decay factor, analogous to that introduced in Section 11.6.1 in the context of $\pi^\pm$ decay. Although the above analysis is rather simplistic, it gives a reasonable estimate of the magnitude of Δm. Taking the charm quark mass to be 1.3 GeV, Equation (14.52) gives the predicted value of $\Delta m \sim 5 \times 10^{-15}\,\text{GeV}$, which is within a factor of two of the observed value. The smallness of Δm is due to the presence of the G_F^2 term from the two exchanged W bosons in the box diagram.

The Standard Model interpretation of ε

CP violation in $K^0 \leftrightarrow \overline{K}^0$ mixing arises because the matrix element for $K^0 \to \overline{K}^0$ is not the same as that for $\overline{K}^0 \to K^0$. For example, the matrix elements for $K^0 \to \overline{K}^0$ and $\overline{K}^0 \to K^0$, arising from the exchange of a charm and a top quark, shown in Figure 14.18, are respectively proportional to

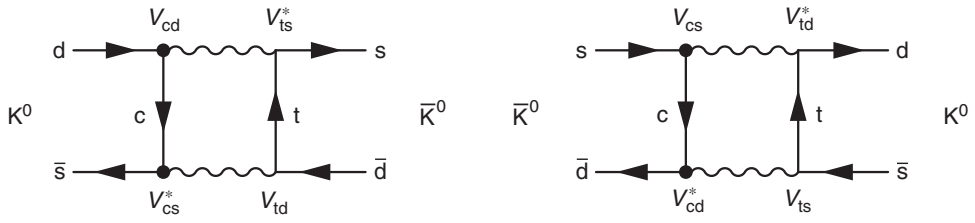

Fig. 14.18 The box diagram for $K^0 \to \overline{K}^0$ involving virtual c and t quarks and the corresponding diagram for $\overline{K}^0 \to K^0$.

$$\mathcal{M}_{12} \propto V_{cd} V_{cs}^* V_{td} V_{ts}^* \quad \text{and} \quad \mathcal{M}_{21} \propto V_{cd}^* V_{cs} V_{td}^* V_{ts} = \mathcal{M}_{12}^*.$$

CP violation in mixing occurs if $\mathcal{M}_{12} \neq \mathcal{M}_{12}^*$. It can be shown (see Problem 14.9) that

$$|\varepsilon| \approx \frac{\Im\mathfrak{m}\{\mathcal{M}_{12}\}}{\sqrt{2}\,\Delta m}.$$

The imaginary part of $\mathcal{M}_{12}$ can be expressed in terms of the possible combinations of exchanged u, c, t quarks in the box diagrams,

$$\Im\mathfrak{m}\{\mathcal{M}_{12}\} = \sum_{q,q'} \mathcal{A}_{qq'}\, \Im\mathfrak{m}\,(V_{qd} V_{qs}^* V_{q'd} V_{q's}^*),$$

where the parameters $\mathcal{A}_{qq'}$ are constants that depend on the masses of the exchanged quarks. In the Wolfenstein parameterisation of the CKM matrix given in (14.9), the imaginary elements of the CKM matrix are V_{td} and V_{ub}. Since V_{ub} is not relevant for kaon mixing, CP violation in neutral kaon mixing is associated with box diagrams involving at least one top quark, and therefore

$$|\varepsilon| \propto \mathcal{A}_{ut}\, \Im\mathfrak{m}\,(V_{ud} V_{us}^* V_{td} V_{ts}^*) + \mathcal{A}_{ct}\, \Im\mathfrak{m}\,(V_{cd} V_{cs}^* V_{td} V_{ts}^*) + \mathcal{A}_{tt}\, \Im\mathfrak{m}\,(V_{td} V_{ts}^* V_{td} V_{ts}^*). \tag{14.53}$$

Writing the elements of the CKM matrix in terms of A, λ, ρ and η of the Wolfenstein parametrisation (14.9), it can be shown that (see Problem 14.10)

$$|\varepsilon| \propto \eta(1 - \rho + \text{constant}).$$

Hence the measurement of a non-zero value of $|\varepsilon|$ implies that $\eta \neq 0$ and provides an experimental constraint on the possible values of the parameters η and ρ.

14.6 B-meson physics

The oscillations of neutral mesons are not confined to kaons, they have also been observed for the heavy neutral meson systems,

$$\mathrm{B}^0(\bar{\mathrm{b}}\mathrm{d}) \leftrightarrow \overline{\mathrm{B}}^0(\mathrm{b}\bar{\mathrm{d}}), \quad \mathrm{B}_\mathrm{s}^0(\bar{\mathrm{b}}\mathrm{s}) \leftrightarrow \overline{\mathrm{B}}_\mathrm{s}^0(\mathrm{b}\bar{\mathrm{s}}) \quad \text{and} \quad \mathrm{D}^0(\bar{\mathrm{c}}\mathrm{u}) \leftrightarrow \overline{\mathrm{D}}^0(\mathrm{c}\bar{\mathrm{u}}).$$

In particular, the results from the studies of the $\mathrm{B}^0(\bar{\mathrm{b}}\mathrm{d})$ and $\overline{\mathrm{B}}^0(\mathrm{b}\bar{\mathrm{d}})$ mesons by the BaBar and Belle experiments have provided crucial information on the CKM matrix and CP violation. The mathematical treatment of the oscillations of the $\mathrm{B}^0(\bar{\mathrm{b}}\mathrm{d}) \leftrightarrow \overline{\mathrm{B}}^0(\mathrm{b}\bar{\mathrm{d}})$ system follows closely that developed for the neutral kaon system. However, because the B^0 and $\overline{\mathrm{B}}^0$ are relatively massive, $m(\mathrm{B}) \sim 5.3\,\mathrm{GeV}$, they have a large number of possible decay modes; to date, over 400 have been observed; see Beringer *et al.* (2012). Of these decay modes, relatively few are common to both the B^0 and $\overline{\mathrm{B}}^0$. Consequently, the interference between the decays of

the B^0 and $\overline{B}^0$ is small. Because of this, it can be shown (see the following starred section) that $B^0 \leftrightarrow \overline{B}^0$ oscillations can be described by a single angle β and that the physical eigenstates of the neutral B-meson system are

$$|B_L\rangle = \frac{1}{\sqrt{2}}\left[|B^0\rangle + e^{-i2\beta}|\overline{B}^0\rangle\right] \quad \text{and} \quad |B_H\rangle = \frac{1}{\sqrt{2}}\left[|B^0\rangle - e^{-i2\beta}|\overline{B}^0\rangle\right]. \tag{14.54}$$

The B_L and B_H are respectively a lighter and heavier state with almost identical lifetimes; again the mass difference $m(B_L) - m(B_H)$ is very small.

14.6.1 *B-meson mixing

The treatment of B-mixing given here, makes a number of approximations to simplify the discussion in order to focus on the main physical concepts. The physical neutral B-meson states are the eigenstates of the overall Hamiltonian of the B^0 and $\overline{B}^0$ system, analogous to the kaon states discussed in Section 14.4.3. There are a large number of B-meson decay modes, of which only a few are common to both the B^0 and $\overline{B}^0$, and the contribution to the effective Hamiltonian of (14.25) from the interference between the decays of the B^0 and $\overline{B}^0$ can be neglected, $\Gamma_{12} = \Gamma_{21}^* \approx 0$. In this case

$$\mathcal{H} \approx \begin{pmatrix} M - \frac{i}{2}\Gamma & M_{12} \\ M_{12}^* & M - \frac{i}{2}\Gamma \end{pmatrix}, \tag{14.55}$$

where M_{12} is due to the box diagrams for $B^0 \leftrightarrow \overline{B}^0$ mixing. The eigenvalues of (14.55), which determine the masses and lifetimes of the physical states, are

$$\lambda_H = m_H + \tfrac{1}{2}i\Gamma_H \approx M + |M_{12}| - \tfrac{1}{2}i\Gamma,$$
$$\lambda_L = m_L + \tfrac{1}{2}i\Gamma_L \approx M - |M_{12}| - \tfrac{1}{2}i\Gamma.$$

leading to a heavier state B_H and a lighter state B_L with masses

$$m_H = M + |M_{12}| \quad \text{and} \quad m_L = M - |M_{12}|. \tag{14.56}$$

Because the interference term Γ_{12} is sufficiently small that it can be neglected, the imaginary parts of λ_H and λ_L are the same. Consequently, the B_H and B_L have approximately the same lifetime, which is measured to be

$$\Gamma_H \approx \Gamma_L \approx \Gamma \approx 4.3 \times 10^{-13}\,\text{GeV}.$$

The corresponding physical eigenstates of the effective Hamiltonian are

$$|B_L\rangle = \frac{1}{\sqrt{1+|\xi|^2}}(|B^0\rangle + \xi|\overline{B}^0\rangle) \quad \text{and} \quad |B_H\rangle = \frac{1}{\sqrt{1+|\xi|^2}}(|B^0\rangle - \xi|\overline{B}^0\rangle), \tag{14.57}$$

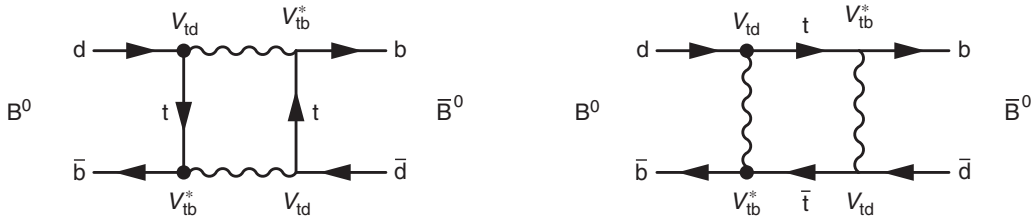

Fig. 14.19 The dominant box diagrams for $B^0 \leftrightarrow \overline{B}^0$ mixing.

where ξ is given by (14.29),

$$\xi = \left(\frac{M_{12}^* - \frac{i}{2}\Gamma_{12}^*}{M_{12} - \frac{i}{2}\Gamma_{12}} \right)^{\frac{1}{2}} \approx \frac{M_{12}^*}{|M_{12}|}, \tag{14.58}$$

from which it follows that $|\xi| \approx 1$.

In $K^0 \leftrightarrow \overline{K}^0$ mixing, the contributions from different flavours of virtual quarks in the box diagrams are of a similar order of magnitude. Here, because $|V_{tb}| \gg |V_{ts}| > |V_{td}|$, only the box diagrams involving two top quarks, shown in Figure 14.19, contribute significantly to the mixing process and

$$M_{12}^* \propto (V_{td} V_{tb}^*)^2.$$

In the Wolfenstein parametrisation of the CKM matrix (14.9), V_{tb} is real and thus

$$\xi = \frac{M_{12}^*}{|M_{12}|} = \frac{(V_{td} V_{tb}^*)^2}{|(V_{td} V_{tb}^*)^2|} = \frac{V_{td}^2}{|V_{td}^2|}. \tag{14.59}$$

By writing V_{td} as

$$V_{td} = |V_{td}| e^{-i\beta},$$

the expression for ξ given in (14.59) is simply

$$\xi = e^{-i2\beta}.$$

Hence, the physical neutral B-meson states of (14.57) are

$$|B_L\rangle = \frac{1}{\sqrt{2}} \left(|B^0\rangle + e^{-i2\beta} |\overline{B}^0\rangle \right) \quad \text{and} \quad |B_H\rangle = \frac{1}{\sqrt{2}} \left(|B^0\rangle - e^{-i2\beta} |\overline{B}^0\rangle \right). \tag{14.60}$$

From (14.56), it can be seen that the mass difference

$$\Delta m_d = m(B_H) - m(B_L) = 2|M_{12}| \propto |(V_{td} V_{tb}^*)^2|. \tag{14.61}$$

Because $V_{tb} \approx 1$, it follows that the $B_H - B_L$ mass difference is proportional to $|V_{td}^2|$. Consequently, the measurement of Δm_d in $B^0 \leftrightarrow \overline{B}^0$ mixing provides a way of determining $|V_{td}|$.

14.6.2 Neutral B-meson oscillations

The mathematical description of the phenomenon of B-meson oscillations follows that developed for the kaon system. Suppose a $\mathrm{B}^0(\bar{\mathrm{b}}\mathrm{d})$ is produced at a time $t = 0$, such that $|\mathrm{B}(0)\rangle = |\mathrm{B}^0\rangle$. Then from (14.60), the flavour state B^0 can be expressed in terms of the physical B_H and B_L mass eigenstates

$$|\mathrm{B}^0\rangle = \tfrac{1}{\sqrt{2}}\left(|\mathrm{B}_L\rangle + |\mathrm{B}_H\rangle\right).$$

The wavefunction evolves according to the time dependence of the physical states,

$$|\mathrm{B}(t)\rangle = \tfrac{1}{\sqrt{2}}\left[\theta_L(t)|\mathrm{B}_L\rangle + \theta_H(t)|\mathrm{B}_H\rangle\right], \tag{14.62}$$

where the time dependencies of the physical states are

$$\theta_L = e^{-\Gamma t/2}e^{-im_L t} \quad \text{and} \quad \theta_H = e^{-\Gamma t/2}e^{-im_H t}.$$

Equation (14.62) can be expressed in terms of the flavour eigenstates using (14.60),

$$|\mathrm{B}(t)\rangle = \tfrac{1}{2}\left[(\theta_L + \theta_H)|\mathrm{B}^0\rangle + e^{-i2\beta}(\theta_L - \theta_H)|\overline{\mathrm{B}}^0\rangle\right] = \tfrac{1}{2}\left[\theta_+|\mathrm{B}^0\rangle + \xi\theta_-|\overline{\mathrm{B}}^0\rangle\right], \tag{14.63}$$

where $\theta_\pm = \theta_L \pm \theta_H$ and $\xi = e^{-2i\beta}$. By writing $m_L = M - \Delta m_\mathrm{d}/2$ and $m_H = M + \Delta m_\mathrm{d}/2$,

$$\theta_\pm(t) = e^{-\Gamma t/2}e^{-iMt} \times \left[e^{i\Delta m_\mathrm{d} t/2} \pm e^{-i\Delta m_\mathrm{d} t/2}\right], \tag{14.64}$$

from which it follows that θ_+ and θ_- are given by

$$\theta_+ = 2e^{-\Gamma t/2}e^{-iMt}\cos\left(\frac{\Delta m_\mathrm{d} t}{2}\right) \quad \text{and} \quad \theta_- = 2ie^{-\Gamma t/2}e^{-iMt}\sin\left(\frac{\Delta m_\mathrm{d} t}{2}\right).$$

The probabilities of the state decaying as a $|\mathrm{B}^0\rangle$ or a $|\overline{\mathrm{B}}^0\rangle$ are therefore

$$\begin{aligned} P(\mathrm{B}^0_{t=0} \to \mathrm{B}^0) &= |\langle \mathrm{B}(t)|\mathrm{B}^0\rangle|^2 = \tfrac{1}{4}e^{-\Gamma t}|\theta_+|^2 = e^{-\Gamma t}\cos^2\left(\tfrac{1}{2}\Delta m_\mathrm{d} t\right), \\ P(\mathrm{B}^0_{t=0} \to \overline{\mathrm{B}}^0) &= |\langle \mathrm{B}(t)|\overline{\mathrm{B}}^0\rangle|^2 = \tfrac{1}{4}e^{-\Gamma t}|\xi\theta_-|^2 = |\xi|^2 e^{-\Gamma t}\sin^2\left(\tfrac{1}{2}\Delta m_\mathrm{d} t\right). \end{aligned} \tag{14.65}$$

The corresponding expressions for a state that was produced as a $\overline{\mathrm{B}}^0$ are

$$P(\overline{\mathrm{B}}^0_{t=0} \to \overline{\mathrm{B}}^0) = e^{-\Gamma t}\cos^2\left(\tfrac{1}{2}\Delta m_\mathrm{d} t\right) \text{ and } P(\overline{\mathrm{B}}^0_{t=0} \to \mathrm{B}^0) = \left|\frac{1}{\xi}\right|^2 e^{-\Gamma t}\sin^2\left(\tfrac{1}{2}\Delta m_\mathrm{d} t\right).$$

Because the contribution to the effective Hamiltonian for the neutral B-meson system from the interference between B^0 and $\overline{\mathrm{B}}^0$ decays can be neglected, $|\xi| = |e^{-i2\beta}| = 1$ and therefore

$$P(\overline{\mathrm{B}}^0_{t=0} \to \overline{\mathrm{B}}^0) \approx P(\mathrm{B}^0_{t=0} \to \mathrm{B}^0) \quad \text{and} \quad P(\overline{\mathrm{B}}^0_{t=0} \to \mathrm{B}^0) \approx P(\mathrm{B}^0_{t=0} \to \overline{\mathrm{B}}^0).$$

Consequently, it is very hard to observe CP violation in neutral B-meson *mixing*. Nevertheless, $\mathrm{B}^0 \leftrightarrow \overline{\mathrm{B}}^0$ oscillations can be utilised to measure Δm_d, which from (14.61) provides a measurement of $|V_\mathrm{td}|$.

14.6.3 The BaBar and Belle experiments

The BaBar (1999–2008) and Belle (1999–2010) experiments were designed to provide precise measurements of CP violation in the neutral B-meson system. The experiments utilised the high-luminosity PEP2 and KEKB e^+e^- colliders at SLAC in California and KEK in Japan. To produce very large numbers of $B^0\overline{B}^0$ pairs, the colliders operated at a centre-of-mass energy of 10.58 GeV, which corresponds to the mass of the $\Upsilon(4S)$ $b\bar{b}$ resonance. The $\Upsilon(4S)$ predominantly decays by either $\Upsilon(4S) \to B^+B^-$ or $\Upsilon(4S) \to B^0\overline{B}^0$, with roughly equal branching ratios. The masses of the charged and neutral B-mesons are 5.279 GeV, and therefore they are produced almost at rest in the centre-of-mass frame of the $\Upsilon(4S)$. Because the lifetimes of the neutral B-mesons are short ($\tau = 1.519 \times 10^{-12}$ s) and they are produced with relatively low velocities, they travel only a short distance in the centre-of-mass frame before decaying. Consequently, in the centre-of-mass frame it would be hard to separate the decays of two B-mesons produced in $e^+e^- \to \Upsilon(4S) \to B^0\overline{B}^0$. For this reason, the PEP2 and KEKB colliders operated as asymmetric b-factories, where the electron beam energy was higher than that of the positron beam. For example, PEP2 collided a 9 GeV electron beam with a 3.1 GeV positron beam. Owing to the asymmetric beam energies, the $\Upsilon(4S)$ is boosted along the beam axis; at the PEP2 collider the $\Upsilon(4S)$ is produced with $\beta\gamma = 0.56$. As a result of this boost, the mean distance between the two B-meson decay vertices in the beam direction is increased to $\Delta z \sim 200\,\mu$m. This separation is large enough for the two B-meson decay vertices to be resolved using a high-precision silicon vertex detector, as described in Section 1.3.1.

The oscillations of B-mesons can be studied through their leptonic decays,

$$B^0(\bar{b}d) \to D^-(\bar{c}d)\,\mu^+\,\nu_\mu \quad \text{and} \quad \overline{B}^0(b\bar{d}) \to D^+(c\bar{d})\,\mu^-\,\overline{\nu}_\mu.$$

The sign of the lepton identifies the B-meson flavour state, since the decays $B^0 \to D^+\mu^-\overline{\nu}_\mu$ and $\overline{B}^0 \to D^-\mu^+\nu_\mu$ do not occur. After production in $e^+e^- \to B^0\overline{B}^0$, the two B-mesons propagate as a coherent state. When one of the B-mesons decays into a particular flavour eigenstate, the overall wavefunction collapses, fixing the flavour state of the other B-meson. For example, Figure 14.20 illustrates the case where at $t = 0$ one of the B-mesons is observed to decay to $D^+\mu^-\overline{\nu}_\mu$, tagging it as a $\overline{B}^0$. At this instant in time, the second B-meson corresponds to a pure B^0 state, $|B(0)\rangle = |B^0\rangle$. The wavefunction of the second B-meson then evolves according to (14.63). When the second B-meson decays Δt later, the charge sign of the observed lepton tags the flavour eigenstate in which the decay occurred. Thus $B^0 \leftrightarrow \overline{B}^0$ oscillations can be studied by measuring the rates where the two B-meson decays are the same flavour, B^0B^0 and $\overline{B}^0\overline{B}^0$, or are of opposite flavour, $B^0\overline{B}^0$. The same flavour (SF) decays give like-sign leptons, $\mu^+\mu^+$ or $\mu^-\mu^-$, and the opposite flavour (OF) decays give opposite-sign leptons, $\mu^+\mu^-$. The relative rates depend on the

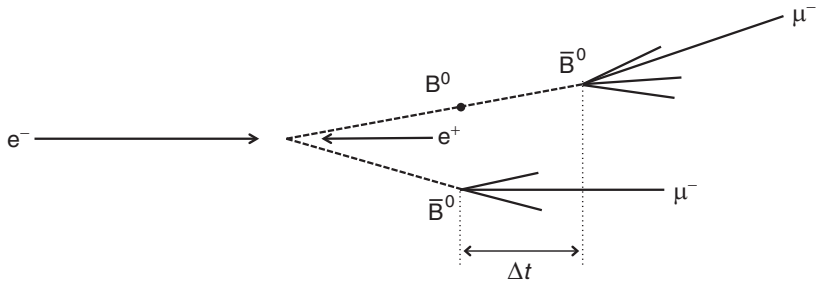

Fig. 14.20 The process $e^+e^- \to B^0\overline{B}^0$ followed by two same-flavour (SF) leptonic $\overline{B}^0$ decays, following $B^0 \to \overline{B}^0$ oscillation.

time between the two decays Δt. Because the B-mesons are produced almost at rest in the centre-of-mass frame, the proper time between the two decays is given by $\Delta t = \Delta z/\beta\gamma c$, where β and γ are determined from the known velocity of the Υ.

The mass difference $\Delta m_\mathrm{d} = m(\mathrm{B}_H) - m(\mathrm{B}_L)$ is determined from the lepton flavour asymmetry $A(\Delta t)$ defined as

$$A(\Delta t) = \frac{N_{OF} - N_{SF}}{N_{SF} + N_{OF}},$$

where N_{OF} is the number of observed opposite flavour decays and N_{SF} is the corresponding number of same flavour decays. The observed asymmetry can be expressed in terms of the oscillation probabilities as

$$A(\Delta t) = \frac{[P(\mathrm{B}^0_{t=0} \to \mathrm{B}^0) + P(\overline{\mathrm{B}}^0_{t=0} \to \overline{\mathrm{B}}^0)] - [P(\mathrm{B}^0_{t=0} \to \overline{\mathrm{B}}^0) + P(\overline{\mathrm{B}}^0_{t=0} \to \mathrm{B}^0)]}{[P(\mathrm{B}^0_{t=0} \to \mathrm{B}^0) + P(\overline{\mathrm{B}}^0_{t=0} \to \overline{\mathrm{B}}^0)] + [P(\mathrm{B}^0_{t=0} \to \overline{\mathrm{B}}^0) + P(\overline{\mathrm{B}}^0_{t=0} \to \mathrm{B}^0)]},$$

which, using (14.65) and the subsequent relations, gives

$$A(\Delta t) = \cos^2\left(\tfrac{1}{2}\Delta m_\mathrm{d} t\right) - \sin^2\left(\tfrac{1}{2}\Delta m_\mathrm{d} t\right) = \cos\left(\Delta m_\mathrm{d} t\right). \tag{14.66}$$

Figure 14.21 shows the measurement of $A(\Delta t)$ from the Belle experiment. The data do not follow the pure cosine form of (14.66) due to a number of experimental effects, including the presence of background, the misidentification of the lepton charge and the experimental Δt resolution. Nevertheless, the effects of $\mathrm{B}^0 \leftrightarrow \overline{\mathrm{B}}^0$ oscillations are clearly observed. When combined, the results from the BaBar and Belle experiments give

$$\Delta m_\mathrm{d} = (0.507 \pm 0.005)\,\mathrm{ps}^{-1} \equiv (3.34 \pm 0.03) \times 10^{-13}\,\mathrm{GeV}.$$

From (14.61) and the knowledge that $V_\mathrm{tb} \approx 1$, the measured value of Δm_d can be interpreted as a measurement of

$$|V_\mathrm{td}| = (8.4 \pm 0.6) \times 10^{-3}.$$

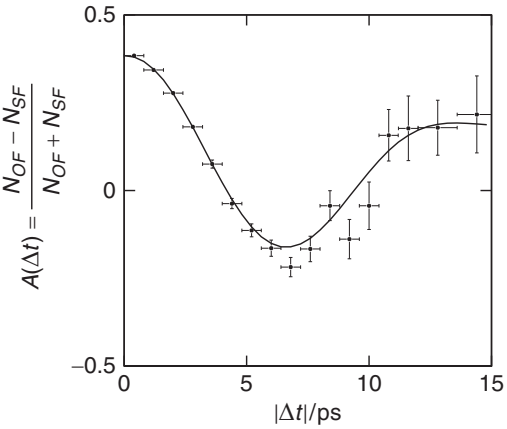

Fig. 14.21 The Belle measurement of $A_{\Delta t}$. The line represents a fit to the data including contributions from background and the effects of experimental resolution. Adapted from Abe *et al.* (2005).

In a similar manner, $|V_{\rm ts}|$ can be extracted from the measurements of oscillations in the $\mathrm{B_s^0}(\mathrm{\bar{b}s}) \leftrightarrow \mathrm{\overline{B}_s^0}(\mathrm{b\bar{s}})$ system from the CDF and LHCb experiments, see Abulencia *et al.* (2006) and Aaij *et al.* (2012). When the results from these two experiments are averaged they give $\Delta m_{\rm s} = 17.72 \pm 0.04\,\mathrm{ps}^{-1}$. Taking $V_{\rm tb} \approx 1$ this result leads to

$$|V_{\rm ts}| = (4.3 \pm 0.3) \times 10^{-2}.$$

14.6.4 CP violation in the B-meson system

In general, CP violation can be observed as three distinct effects:

(i) direct CP violation in decay such that $\Gamma(A \to X) \neq \Gamma(\overline{A} \to \overline{X})$, as parameterised by ε' in the neutral kaon system;
(ii) CP violation in the mixing of neutral mesons as parameterised by ε in the kaon system;
(iii) CP violation in the interference between decays to a common final state f with and without mixing, for example $\mathrm{B^0} \to f$ and $\mathrm{B^0} \to \mathrm{\overline{B}^0} \to f$.

In the Standard Model, the effects of CP violation in $\mathrm{B^0} \leftrightarrow \mathrm{\overline{B}^0}$ mixing is small. Nevertheless, CP-violating effects in the interference between decays $\mathrm{B^0} \to f$ and $\mathrm{B^0} \to \mathrm{\overline{B}^0} \to f$ can be relatively large and have been studied extensively by the BaBar and Belle experiments in a number of final states; here the decay $\mathrm{B} \to \mathrm{J/\psi\,K}_S$ is used to illustrate the main ideas. To simplify the notation, the $\mathrm{J/\psi}$ meson is written simply as ψ.

The ψ charmonium ($\mathrm{c\bar{c}}$) state has $J^P = 1^-$ and is a CP eigenstate with $CP = +1$. Neglecting CP violation in neutral kaon mixing, the K_S is to a good approximation,

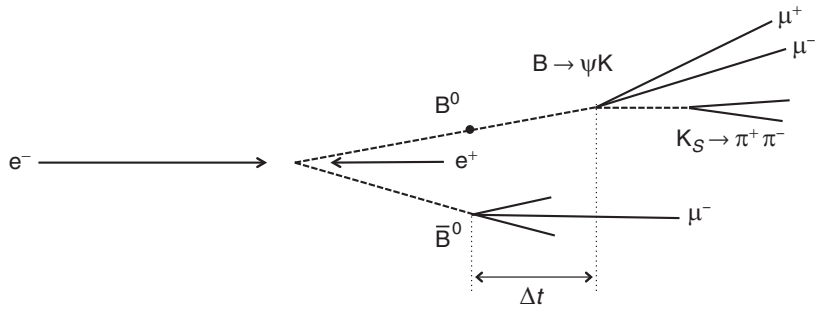

Fig. 14.22 The process $e^+e^- \to B^0\overline{B}^0$ where the leptonic decay tags the flavour of the other B-meson as being a B^0 that subsequently decays to a $\psi\, K_S$. In this illustrative example, $\psi \to \mu^+\mu^-$ and $K_S \to \pi^+\pi^-$.

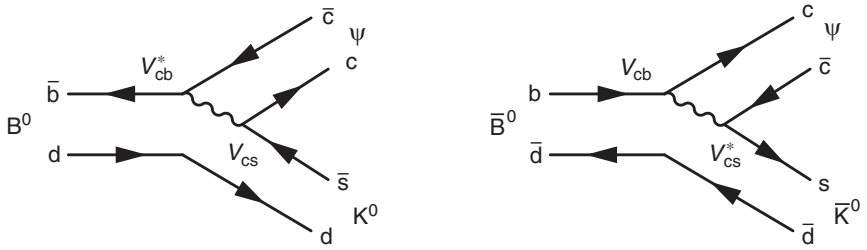

Fig. 14.23 The Feynman diagrams for $B^0 \to \psi\, K^0$ and $\overline{B}^0 \to \psi\, \overline{K}^0$.

the $CP = +1$ eigenstate of the neutral kaon system with $J^P = 0^-$. Since the B^0 and $\overline{B}^0$ are spin-0 mesons, the decays $B^0 \to \psi\, K_S$ and $\overline{B}^0 \to \psi\, K_S$ must result in an $\ell = 1$ orbital angular momentum state. Therefore the CP state of the combined $\psi\, K_S$ system is

$$CP(\psi\, K_S) = CP(\psi) \times CP(K_S) \times (-1)^\ell = (+1)(+1)(-1) = -1.$$

Similarly, the decay $B \to \psi\, K_L$ occurs in a CP-even state, $CP(\psi\, K_L) = +1$.

Figure 14.22 shows the topology of a typical neutral B-meson decay to $\psi\, K_S$. In this example, the charge of the muon in the leptonic $\overline{B}^0 \to D^+\mu^-\overline{\nu}_\mu$ decay tags it as $\overline{B}^0$ and hence at time $t = 0$, the other B-meson is in a B^0 flavour state, $|B(0)\rangle = |B^0\rangle$. The decay to $\psi\, K_S$ can either occur directly by $B^0 \to \psi\, K_S$ or after mixing, $B^0 \to \overline{B}^0 \to \psi\, K_S$. It is the interference between the two amplitudes for these processes, which have different phases, that provides the sensitivity to the CP violating angle β. The $B \to \psi\, K_S$ decays can be identified from the clear experimental signatures, for example $\psi \to \mu^+\mu^-$ and $K_S \to \pi^+\pi^-$.

The $B^0/\overline{B}^0 \to \psi\, K_S$ decays proceed in two stages. First the $B^0/\overline{B}^0$ decays to the corresponding *flavour* eigenstate, $B^0 \to \psi K^0$ and $\overline{B}^0 \to \psi\overline{K}^0$, as shown in Figure 14.23. Subsequently, the neutral kaon system evolves as as a linear combination of the physical K_S and K_L states and then decays to the CP states $K_S\psi$ and $K_L\psi$. CP violation in the interference between $B^0 \to \psi\, K_S$ and $B^0 \to \overline{B}^0 \to \psi\, K_S$ is measurable through the asymmetry,

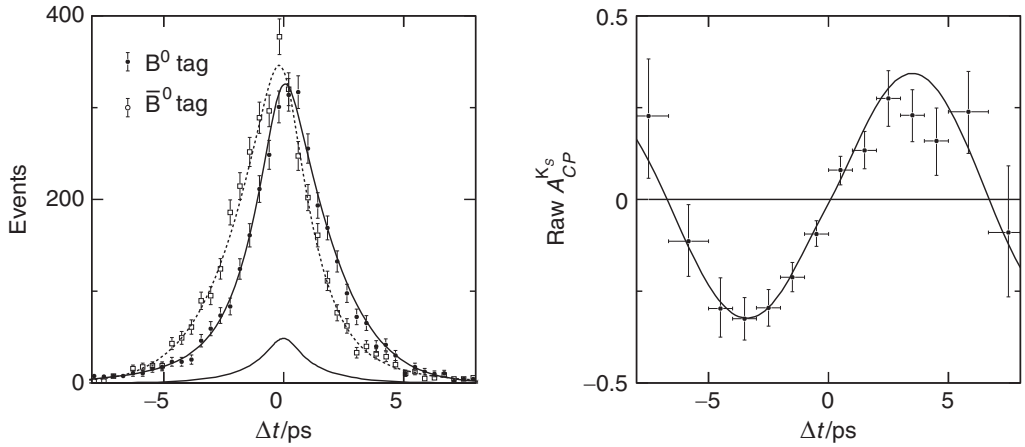

Fig. 14.24 The raw data and distribution of $A_{CP}^{K_S}$ from the BaBar experiment based on a sample of 4×10^8 $\Upsilon(4S) \rightarrow B^0\overline{B}^0$ decays. In the left-hand plot, the small symmetric contribution arises from the background. The lines show the best fit to the data. Adapted from Aubert *et al.* (2007).

$$A_{CP}^{K_S} = \frac{\Gamma(\overline{B}^0_{t=0} \rightarrow \psi K_S) - \Gamma(B^0_{t=0} \rightarrow \psi K_S)}{\Gamma(\overline{B}^0_{t=0} \rightarrow \psi K_S) + \Gamma(B^0_{t=0} \rightarrow \psi K_S)} = \sin(\Delta m_d t)\ \sin(2\beta). \qquad (14.67)$$

Figure 14.24 shows the experimental data from the BaBar experiment. The left-hand plot shows the raw numbers of observed decays to ψK_S, from both events that were tagged as B^0 or $\overline{B}^0$, plotted as a function of Δt. Here Δt is the difference in the proper time of the tagged $B^0/\overline{B}^0$ semi-leptonic decay and the observed $B \rightarrow \psi K_S$ decay. The curves show the expected distributions including a symmetric background contribution from other B-meson decays. The right-hand plot of Figure 14.24 shows the raw asymmetry obtained from these data. This has the expected sinusoidal form of (14.67) and the amplitude provides a measurement of $\sin(2\beta)$,

$$\sin(2\beta) = 0.685 \pm 0.032.$$

This observation of a non-zero value of $\sin(2\beta)$ is a direct manifestation of CP violation in the B-meson system. The Belle experiment (see Adachi *et al.* (2012)) measured $\sin(2\beta) = 0.670 \pm 0.032$.

14.7 CP violation in the Standard Model

There is now a wealth of experimental data on CP violation associated with the weak interactions of quarks. This chapter has focussed on the observations of CP violation in $K^0 - \overline{K}^0$ mixing and in the interference between the amplitudes for $B^0 \rightarrow J/\psi K_S$ and $B^0 \rightarrow \overline{B}^0 \rightarrow J/\psi K_S$ decays. Direct CP violation in the decays of

kaons and B-mesons has also been observed, for example, as a difference between the rates $\Gamma(\overline{B}^0 \to K^-\pi^+)$ and $\Gamma(B^0 \to K^+\pi^-)$.

In the Standard Model, CP violation in the weak interactions of hadrons is described by the single irreducible complex phase in the CKM matrix. In the Wolfenstein parametrisation of (14.9), CP violation is associated with the parameter η. To $O(\lambda^4)$, the parameter η appears only in V_{ub} and V_{td}, with

$$V_{ub} \approx A\lambda^3(\rho - i\eta) \quad \text{and} \quad V_{td} \approx A\lambda^3(1 - \rho - i\eta).$$

The measurements of non-zero values of $|\varepsilon|$ and $\sin(2\beta)$ separately imply that $\eta \neq 0$. However, it is only when the experimental measurements are combined, that the values of ρ and η can be determined.

In the Standard Model, the CKM matrix is unitary, $V^\dagger V = I$. This property places constraints on the possible values of the different elements of the CKM matrix. These constraints are usually expressed in terms of unitarity triangles. For example, the unitarity of the CKM matrix implies that

$$V_{ud}V_{ub}^* + V_{cd}V_{cb}^* + V_{td}V_{tb}^* = 0. \tag{14.68}$$

In the Wolfenstein parametrisation, of these six CKM matrix elements, V_{ud}, V_{tb}, V_{cd} and V_{cb} are all real and only V_{cd} is negative. Hence (14.68) can be divided by $V_{cd}V_{cb}$ to give

$$1 - \frac{|V_{ud}|}{|V_{cd}||V_{cb}|}V_{ub}^* - \frac{|V_{tb}|}{|V_{cd}||V_{cb}|}V_{td} = 0. \tag{14.69}$$

Since V_{ub}^* and V_{td} are complex, $V_{ub}^* = A\lambda^3(\rho + i\eta)$ and $V_{td} = A\lambda^3(1 - \rho - i\eta)$, the unitarity relation of (14.69) is a vector equation in the complex ρ–η plane, with the three vectors forming the closed triangle, as shown in Figure 14.25a.

From $V_{td} = |V_{td}|e^{-i\beta} = A\lambda^3(1 - \rho - i\eta)$, it can be seen that

$$\beta = \arg(1 - \rho + i\eta) \quad \text{or equivalently} \quad \tan\beta = \frac{\eta}{1 - \rho}.$$

Consequently, the angle β corresponds to the internal angle of the unitarity triangle shown in Figure 14.25a. Therefore, the measurement of $\sin(2\beta)$ described previously constrains the angle between two of the sides of the unitarity triangle as shown in Figure 14.25b, which also shows the constraint in the ρ–η plane obtained from the measurement of $|\varepsilon|$ in neutral kaon mixing,

$$|\varepsilon| \propto \eta(1 - \rho + \text{constant}).$$

The measurement of Δm_d determines $|V_{td}|$. When this is combined with the knowledge that $|V_{tb}| \approx 1$ and the measurements of $|V_{cd}|$ and $|V_{cb}|$ described in Section 14.3, it constrains of the length of the upper side of the unitarity triangle, as shown in Figure 14.25b.

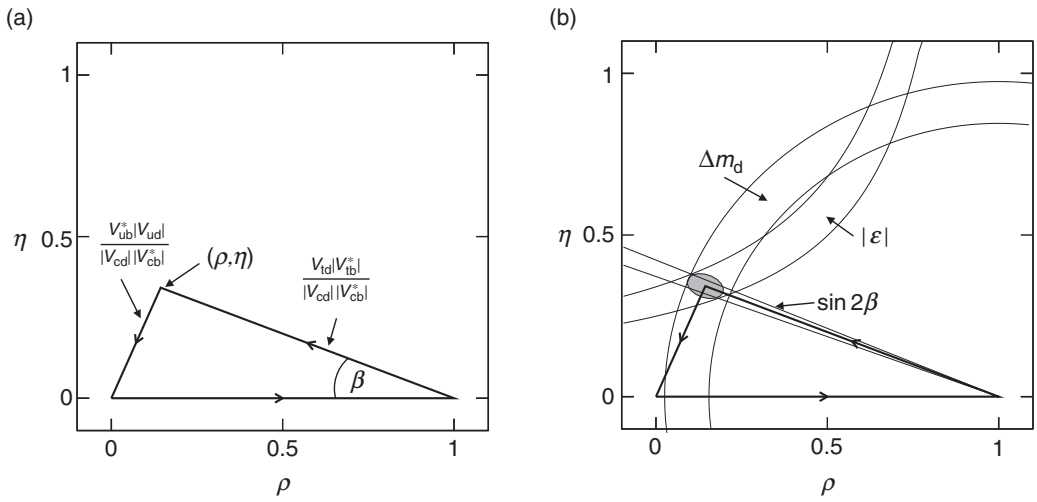

Fig. 14.25 (a) The unitarity relation, $V_{ud}V_{ub}^* + V_{cd}V_{cb}^* + V_{td}V_{tb}^* = 0$, shown in the ρ–η plane. (b) The constraints from the measurements of $|\varepsilon|$, Δm_d and $\sin 2\beta$. The shaded ellipse shows the combination of these constraints that give a measurement of η and ρ.

The experimental constraints from the measurements of $|\varepsilon|$, $\sin(2\beta)$ and Δm_d are consistent with a common point in the ρ–η plane, as indicated by the ellipse in Figure 14.25b, thus providing experimental confirmation of the unitarity relation $V_{ud}V_{ub}^* + V_{cd}V_{cb}^* + V_{td}V_{tb}^* = 0$. From a global fit to these and other results (see Beringer *et al.* (2012)) the Wolfenstein parameters are determined to be

$$\lambda = 0.2253 \pm 0.0007,\ A = 0.811^{+0.022}_{-0.012},\ \rho = 0.13 \pm 0.02,\ \eta = 0.345 \pm 0.014.$$

The experimental measurements described in this chapter provide a strong test of the Standard Model prediction that the unitarity triangle of (14.69) is closed. Any deviation from this prediction would indicate physics beyond the Standard Model. To date, all measurements in the quark flavour sector are consistent a unitary CKM matrix, where the observed CP violation is described by a single complex phase.

Whilst the Standard Model provides an explanation of the observed CP violation in the quark sector, this is not sufficient to explain the matter–antimatter asymmetry in the Universe. There are suggestions that CP violation in the lepton sector during the early evolution of the Universe might account for the observed matter-antimatter asymmetry. However, it is also possible that there are as yet undiscovered CP violating processes beyond the Standard Model. In the coming years the LHCb experiment at the LHC and the Belle II experiment at KEK will probe CP violation in the quark sector with ever increasing precision and may shed further light on this important question.

Summary

CP violation is an essential part of our understanding of particle physics. In the Standard Model it can be accommodated in the irreducible complex phases in the PMNS and CKM matrices. In the decays of hadrons, CP violation has been observed in three ways: (i) direct CP violation in decay; (ii) indirect CP violation in the mixing of neutral mesons; and (iii) CP violation in the interference between decays with and without oscillations.

This chapter concentrated on the measurements of oscillations and CP violation in the neutral kaon and neutral B-meson systems. Many of the effects arise from the distinction between the different neutral meson states. For example, neutral kaons are produced in the strong interaction as the flavour eigenstates, $\mathrm{K}^0(\bar{\mathrm{s}}\mathrm{d})$ and $\overline{\mathrm{K}}^0(\mathrm{s}\bar{\mathrm{d}})$, but the physical particles with definite masses and lifetimes are the eigenstates of the overall Hamiltonian of the K^0–$\overline{\mathrm{K}}^0$ system are

$$|\mathrm{K}_S\rangle \propto (1+\varepsilon)|\mathrm{K}^0\rangle + (1-\varepsilon)|\overline{\mathrm{K}}^0\rangle \quad \text{and} \quad |\mathrm{K}_L\rangle \propto (1+\varepsilon)|\mathrm{K}^0\rangle - (1-\varepsilon)|\overline{\mathrm{K}}^0\rangle,$$

where the parameter ε is non-zero only if CP is violated. If CP were conserved in the weak interaction, the physical states would correspond to the CP eigenstates

$$|\mathrm{K}_S\rangle \propto |\mathrm{K}^0\rangle + |\overline{\mathrm{K}}^0\rangle \quad \text{and} \quad |\mathrm{K}_L\rangle \propto |\mathrm{K}^0\rangle - |\overline{\mathrm{K}}^0\rangle.$$

Oscillations arise because neutral mesons are produced as flavour eigenstates and decay as either flavour or CP eigenstates, but propagate as the physical mass eigenstates.

The studies of the neutral mesons and their oscillations, provide constraints on the values of the elements of the CKM matrix and allow CP violation to be studied in the quark sector. To date, all such experimental measurements are consistent with the Standard Model predictions from the single complex phase in the unitary CKM matrix.

Problems

14.1 Draw the lowest-order Feynman diagrams for the decays

$$\mathrm{K}^0 \to \pi^+\pi^-, \quad \mathrm{K}^0 \to \pi^0\pi^0, \quad \overline{\mathrm{K}}^0 \to \pi^+\pi^- \quad \text{and} \quad \overline{\mathrm{K}}^0 \to \pi^0\pi^0,$$

and state how the corresponding matrix elements depend on the Cabibbo angle θ_c.

14.2 Draw the lowest-order Feynman diagrams for the decays

$$B^0 \to D^- \pi^+, \quad B^0 \to \pi^+ \pi^- \quad \text{and} \quad B^0 \to J/\psi\, K^0,$$

and place them in order of decreasing decay rate.

The flavour content of the above mesons is $B^0(d\bar{b})$, $D^-(d\bar{c})$, $J/\psi(c\bar{c})$ and $K^0(d\bar{s})$.

14.3 Draw the lowest-order Feynman diagrams for the weak decays

$$D^0(c\bar{u}) \to K^-(s\bar{u}) + \pi^+(u\bar{d}) \quad \text{and} \quad D^0(c\bar{u}) \to K^+(u\bar{s}) + \pi^-(d\bar{u}),$$

and explain the observation that

$$\frac{\Gamma(D^0 \to K^+\pi^-)}{\Gamma(D^0 \to K^-\pi^+)} \approx 4 \times 10^{-3}.$$

14.4 A hypothetical $\bar{T}^0(t\bar{u})$ meson decays by the weak charged-current decay chain,

$$\bar{T}^0 \to W\pi \to (X\pi)\,\pi \to (Y\pi)\,\pi\,\pi \to (Z\pi)\,\pi\,\pi\,\pi.$$

Suggest the most likely identification of the W, X, Y and Z mesons and state why this decay chain would be preferred over the direct decay $\bar{T}^0 \to Z\,\pi$.

14.5 For the cases of two, three and four generations, state:

- **(a)** the number of free parameters in the corresponding $n \times n$ unitary matrix relating the quark flavour and weak states;
- **(b)** how many of these parameters are real and how many are complex phases;
- **(c)** how many of the complex phases can be absorbed into the definitions of phases of the fermions without any physical consequences;
- **(d)** whether CP violation can be accommodated in quark mixing.

14.6 Draw the lowest-order Feynman diagrams for the strong interaction processes

$$\bar{p}p \to K^-\pi^+K^0 \quad \text{and} \quad \bar{p}p \to K^+\pi^-\bar{K}^0.$$

14.7 In the neutral kaon system, time-reversal violation can be expressed in terms of the asymmetry

$$A_T = \frac{\Gamma(\bar{K}^0 \to K^0) - \Gamma(K^0 \to \bar{K}^0)}{\Gamma(\bar{K}^0 \to K^0) + \Gamma(K^0 \to \bar{K}^0)}.$$

Show that this is equivalent to

$$A_T = \frac{\Gamma(\bar{K}^0_{t=0} \to \pi^- e^+ \nu_e) - \Gamma(K^0_{t=0} \to \pi^+ e^- \bar{\nu}_e)}{\Gamma(\bar{K}^0_{t=0} \to \pi^- e^+ \nu_e) + \Gamma(K^0_{t=0} \to \pi^+ e^- \bar{\nu}_e)},$$

and therefore

$$A_T \approx 4|\varepsilon| \cos\phi.$$

14.8 The $K_S - K_L$ mass difference can be expressed as

$$\Delta m = m(K_L) - m(K_S) \approx \sum_{q,q'} \frac{G_F^2}{3\pi^2} f_K^2 m_K |V_{qd} V_{qs}^* V_{q'd} V_{q's}^*|\, m_q m_{q'},$$

where q and q′ are the quark flavours appearing in the box diagram. Using the values for the CKM matrix elements given in (14.8), obtain expressions for the relative contributions to Δm arising from the different combinations of quarks in the box diagrams.

14.9 Indirect CP violation in the neutral kaon system is expressed in terms of $\varepsilon = |\varepsilon| e^{j\phi}$. Writing

$$\xi = \frac{1-\varepsilon}{1+\varepsilon} \approx 1 - 2\varepsilon = \left(\frac{M_{12}^* - \frac{j}{2}\Gamma_{12}^*}{M_{12} - \frac{j}{2}\Gamma_{12}} \right)^{\frac{1}{2}},$$

show that

$$\varepsilon \approx \frac{1}{2} \times \left(\frac{(\mathfrak{Im}\{M_{12}\} - \frac{j}{2}\,\mathfrak{Im}\{\Gamma_{12}\})}{M_{12} - \frac{j}{2}\Gamma_{12}} \right)^{\frac{1}{2}} \approx \frac{\mathfrak{Im}\{M_{12}\} - j\,\mathfrak{Im}\{\Gamma_{12}/2\}}{\Delta m - j\Delta\Gamma/2}.$$

Using the knowledge that $\phi \approx 45°$ and the measurements of Δm and $\Delta\Gamma$, deduce that $\mathfrak{Im}\{M_{12}\} \gg \mathfrak{Im}\{\Gamma_{12}\}$ and therefore

$$|\varepsilon| \sim \frac{1}{\sqrt{2}} \frac{\mathfrak{Im}\{M_{12}\}}{\Delta m}.$$

14.10 Using (14.53) and the explicit form of Wolfenstein parametrisation of the CKM matrix, show that

$$|\varepsilon| \propto \eta(1 - \rho + \text{constant}).$$

14.11 Show that the $B^0 - \overline{B}^0$ mass difference is dominated by the exchange of two top quarks in the box diagram.

14.12 Calculate the velocities of the B-mesons produced in the decay at rest of the $\Upsilon(4S) \to B^0\overline{B}^0$.

14.13 Given the lifetimes of the neutral B-mesons are $\tau = 1.53$ ps, calculate the mean distance they travel when produced at the KEKB collider in collisions of 8 GeV electrons and 3.5 GeV positrons.

14.14 From the measured values

$$|V_{ud}| = 0.974\,25 \pm 0.000\,22 \quad \text{and} \quad |V_{ub}| = (4.15 \pm 0.49) \times 10^{-3},$$
$$|V_{cd}| = 0.230 \pm 0.011 \quad \text{and} \quad |V_{cb}| = 0.041 \pm 0.001,$$

calculate the length of the corresponding side of the unitarity triangle in Figure 14.25 and its uncertainty. By sketching this constraint and that from the measured value of β, obtain approximate constraints on the values of ρ and η.